

## **Rationally designed oral vaccines can set an evolutionary trap for *Salmonella* Typhimurium**

Médéric Diard<sup>1,2,\*</sup>, Erik Bakkeren<sup>1</sup>, Daniel Hoces<sup>3</sup>, Verena Lentsch<sup>3</sup>, Markus Arnoldini<sup>3</sup>, Flurina Böhi<sup>1,17</sup>, Kathrin Schumann-Moor<sup>1,19</sup>, Jozef Adamcik<sup>3</sup>, Luca Piccoli<sup>4</sup>, Antonio Lanzavecchia<sup>4</sup>, Beth M. Stadtmueller<sup>5</sup>, Nicholas Donohue<sup>6,18</sup>, Marjan W. van der Woude<sup>6</sup>, Alyson Hockenberry<sup>7,8</sup>, Patrick H. Viollier<sup>9</sup>, Laurent Falquet<sup>10,11</sup>, Daniel Wüthrich<sup>12</sup>, Ferdinando Bonfiglio<sup>13</sup>, Adrian Egli<sup>12,13</sup>, Giorgia Zandomeneghi<sup>14</sup>, Raffaele Mezzenga<sup>3,15</sup>, Otto Holst<sup>16</sup>, Beat H. Meier<sup>14</sup>, Wolf-Dietrich Hardt<sup>1,\*</sup>, Emma Slack<sup>1,3,\*</sup>

Affiliations;

1. Institute for Microbiology, Department of Biology, ETH Zürich, Zürich, Switzerland
2. Biozentrum, University of Basel, Basel, Switzerland
3. Institute for Food, Nutrition and Health, ETH Zurich, Zurich, Switzerland
4. Institute for Research in Biomedicine, Università della Svizzera italiana, Bellinzona, Switzerland
5. Department of Biochemistry, University of Illinois at Urbana-Champaign, Urbana, Illinois USA
6. York Biomedical Research Institute, Hull York Medical School, University of York, York, UK
7. Department of Environmental Microbiology, Eawag, Dübendorf, Switzerland
8. Department of Environmental Sciences, ETH Zürich, Switzerland
9. Microbiology and Molecular Medicine, University of Geneva, Geneva, Switzerland
10. Department of Biology, University of Fribourg, Fribourg, Switzerland
11. Swiss Institute of Bioinformatics, Fribourg, Switzerland
12. Infection Biology, Basel University Hospital, Basel, Switzerland
13. Department of Biomedicine, University of Basel, Basel, Switzerland
14. Institute for Physical Chemistry, ETH Zurich, Zurich, Switzerland
15. ETH Zurich, Department of Materials, Wolfgang-Pauli-Strasse 10, 8093 Zürich.
16. Forschungszentrum Borstel, Borstel, Germany

Current addresses:

17. Department of Molecular Mechanisms of Disease, University of Zurich, Zurich, Switzerland
18. Department of Orthopedics and Trauma, Medical University of Graz, Graz, Austria.
19. University of Zurich, Center of Dental Medicine, Oral Biotechnology & Bioengineering

\*Corresponding authors

### **One sentence summary**

By tracking vaccine-driven *Salmonella* evolution in the intestine, it is possible to rationally design oligovalent oral vaccines that generate an evolutionary trap.

### **Abstract**

Secretory antibody responses (Immunoglobulin A, IgA) against repetitive bacterial surface glycans, such as O-antigens and capsules, can protect against intestinal pathogenic *Enterobacteriaceae*. However, efficacy of such immune responses has been limited by rapid glycan evolution and phase-variation. Here, we track IgA-driven O-antigen variation in *Salmonella* Typhimurium, and use this to assemble an oligovalent oral vaccine which sets an

evolutionary trap. IgA targeting all fitness-neutral O-antigen escape variants of *Salmonella* Typhimurium rapidly selected for mutants with very short O-antigen: a phenotype known to display major fitness costs and virulence attenuation in naive hosts. Evolutionary trap vaccination therefore represents an alternative concept in vaccine design. This approach capitalizes on the inevitable and rapid evolution of bacteria in the gut, and can combine protection of the individual with elimination of virulent enteropathogen reservoirs.

## 1 Main text

2 O-Antigen, the long repetitive glycan portion of lipopolysaccharide(1) (LPS), thickly carpets  
3 the surface of all *Salmonella enterica* subspecies *enterica* serovar Typhimurium (*S.Tm*) (**Fig.**  
4 **S1**) in the gut lumen. These glycans are sufficiently long and uniform to shield all non-  
5 protruding outer membrane proteins (e.g. most membrane channels(2–4)) from antibody  
6 binding(5). Protruding surface appendages, such as flagella or adhesins, do extend through the  
7 O-antigen. However, these are typically only expressed on a subset of the population(6, 7)  
8 such that only a fraction of the bacterial population can ever be clumped by antibodies against  
9 such antigens(8, 9). High-affinity intestinal Immunoglobulin A (IgA) against O-antigen,  
10 induced by vaccination or infection(10–12), is therefore the dominant mechanism driving  
11 clumping by enchainment and agglutination(9). As clumped bacteria are unable to  
12 approach the gut wall, this phenomenon provides protection from disease(9, 13, 14).  
13 However, oral vaccines targeting *Escherichia coli*- and *Salmonella* glycans typically generate  
14 weak protection(15–19). The ability of the bacteria to evolve or phase-vary their surface  
15 glycan antigens can be a major contributor to this failure (7, 20, 21).

16  
17 We initially set out to investigate why vaccine-mediated protection fails in non-Typhoidal  
18 *Salmonellosis*. Animals that were vaccinated with a high-dose inactivated oral *S.Tm* vaccine  
19 (PA-*S.Tm*) and infected with wild-type *S.Tm* sporadically developed disease, involving both  
20 intestinal inflammation (quantified via fecal lipocalin 2, **Fig. 1A**) and tissue invasion  
21 (mesenteric lymph node colony forming units (CFU), **Fig. 1B**). Strikingly, disease did not  
22 correlate with IgA titres specific for the wild-type vaccination strain, i.e. occurred despite  
23 robust seroconversion (**Fig. 1C**).

24  
25 As the IgA response was robust, we investigated the phenotype of *S.Tm* clones after growth  
26 in the gut lumen of infected mice. Notably in this model, protection is independent of  
27 intestinal colonization, i.e. the gut luminal *S.Tm* population size is similar in both protected  
28 and diseased mice(9). *S.Tm* clones re-isolated from the feces of "vaccinated but diseased"  
29 mice at day 3 post-infection showed weaker binding to vaccine-induced IgA than *S.Tm* clones  
30 re-isolated from feces of vaccinated protected mice (**Fig. 1D**). This suggested the importance  
31 of another phenomenon driven by IgA: the presence of IgA exerts a strong selection against  
32 the expression of cognate antigens on the surface of luminal *S.Tm*(9). Combined with the  
33 large population size and rapid growth of gut luminal pathogens(9), this generates ideal  
34 conditions for rapid evolution of IgA escape variants.

35  
36 In order to identify changes in surface antigenicity of *S.Tm*, we phenotypically and  
37 genetically characterized the *S.Tm* clones from "vaccinated but diseased" mice. Based on our  
38 observation that protection critically depends on the O-antigen (5, 9), we focused on O-  
39 antigen structure. The *S.Tm* O-antigen is a polymer of -mannose- $\alpha$ -(1→4)rhannose- $\alpha$ -(1→  
40 3)galactose- $\alpha$ -(1→2) with an acetylated  $\alpha$ -(1→3)-linked abequose at the mannose (**Fig 1E**).  
41 Wild-type *S.Tm* strains react strongly to O:12 typing antibodies (recognizing the triose  
42 backbone) and O:5 typing antisera (recognizing the acetylated abequose). Further, *S.Tm* has  
43 multiple options for rapidly generating O-antigen variants. *S.Tm* can shift from O:5 to O:4  
44 (i.e. from an O-antigen with acetylated abequose, to one with non-O-acetylated abequose) by  
45 loss of function mutations in *oafA*, the abequose acetyl transferase. It can further shift  
46 between O:12 (wild-type) and O:12-2 (glucosylated) serotypes by methylation-dependent  
47 expression of a glucosyl transferase operon STM0557-0559 i.e. by phase variation (22, 23).

48 This operon encodes the machinery to add glucose via an  $\alpha$ -(1→4) linkage to the backbone  
49 galactose(22). It should be noted both O-acetylation and backbone-glucosylation represent  
50 major changes in the hydrophobicity or steric properties of the O-antigen repeat unit, which  
51 when extensively polymerized into full-length O-antigen will have major consequences for  
52 antibody binding(24–26).

53

54 We applied multiple techniques to determine the O-antigen structure of evolved *S.Tm* clones.  
55 Flow cytometry with serotyping antibodies (**Fig. 1F**), High Resolution-Magic Angle Spinning  
56 (HR-MAS) on intact bacteria (**Fig. S2A and B**) and <sup>1</sup>H-NMR (27) on purified  
57 lipopolysaccharide (**Fig. S2C**) confirmed the loss of abequose O-acetylation (O:5 to O:4) and  
58 gain of  $\alpha$ -(1→4)-linked glucosylation of galactose (O:12 to O:12-2) in clones from vaccinated  
59 but diseased mice. The emergence of these variants was also observed at later stages during  
60 chronic mouse infections with attenuated *S.Tm* (**Fig. S3**). This was dependent on the presence  
61 of Rag1 and IgA (**Fig. S3**), suggesting that IgA-dependent selective pressure for O-antigen  
62 switching can be generated both by vaccination and by immunity arising naturally during  
63 infection.

64

65 We then explored the underlying genetic mechanisms responsible for altered O-antigen  
66 structure in the evolved clones. We first determined the stability of the observed O-antigen  
67 phenotypes, i.e. whether we would see reversion during cultivation. *In vitro* serial passages of  
68 evolved clones over 5 days revealed that the switch from O:5 to O:4 was a stable, uniform  
69 phenotype (**Fig. 1F and S4A**). Sequencing of O:5-negative evolved clones revealed a  
70 common 7 base-pair contraction of a tandem repeat within the *oafA* open reading frame,  
71 generating a frame-shift and loss of function (**Fig. 2A and B**). Targeted deletion of *oafA*  
72 (*S.Tm* <sup>$\Delta$ oafA</sup>) generated an identical phenotype to the 7 bp deletion (**Fig. 2B**). The same  
73 mutation was detected in deposited genomes of *S. Tm* isolates from swine(28) and is found in  
74 other O:5-negative serovars (e.g., *Salmonella enterica* Heidelberg CP031359.1 "Strain 5"  
75 (**Fig. S5A**)(29)). As there are only two copies of the 7 base-pair motif in the wild type ORF,  
76 the deletion of one 7 base-pair stretch is unlikely to be reversed(30) (**Fig. 2A, Fig. S5A**).  
77 Intriguingly, deposited sequences also indicate copy number variation in a 9bp repeat in the  
78 promoter region of *oafA* (**Fig. S5B**), suggesting a second possible site of microsatellite  
79 instability in this gene.

80

81 When next assessed the stability of O:12 to O:12-2 switching, and its underlying genetic  
82 mechanism. In contrast to O:5, the loss of O:12 was reversible during 3 rounds of serial  
83 passage and both wild-type and evolved clones generated a bimodal staining pattern,  
84 consistent with phase variation (**Fig. 1F and S4A and B, Supplementary movies A and B**,  
85 clones referred to henceforth as O:12<sup>Bimodal</sup>). In line with known epigenetic regulation of the  
86 *gtrABC* operon expression(22), re-sequencing of the O:12<sup>Bimodal</sup> strains revealed no consistent  
87 mutational pattern (supplementary table 3). Instead, a semi-quantitative full-genome  
88 methylation analysis supported that evolved O:12<sup>Bimodal</sup> *S.Tm* clones form mixed populations  
89 based on DNA methylation. Populations of evolved clones presented a high proportion of  
90 chromosomes with a methylation pattern typical of the promoter of *gtrABC* in the ON  
91 state(22, 31, 32) and a minor population in the OFF state (**Fig. 2C**): a situation which is  
92 reversed in the ancestral strain. Targeted deletion of *gtrC* (*S.Tm* <sup>$\Delta$ gtrC</sup>), the serotype-specific  
93 glucosyl transferase of the *gtrABC* operon, abolished the ability of *S.Tm* to switch to an O:12-  
94 bimodal phenotype, even under strong *in vivo* selection (**Fig. S6**). Mathematical modeling of

95 O:12/O:12-2 population sizes for fixed switching rates (supplementary methods, **Fig. S4C-E**),  
96 and comparison of flow cytometry and a *lacZ* transcriptional fusion, suggests that *in vivo*  
97 selection of O:12-2-producing clones by IgA is sufficient to explain their relative proportion  
98 in the O:12<sup>Bimodal</sup> population without needing to infer any change in the switching rate (**Fig.**  
99 **S4**).

100

101 Therefore *S.Tm* clones with an altered O-antigen structure rapidly emerged in vaccinated  
102 mice. In order to quantify how strongly vaccine-induced IgA can select for O-antigen  
103 variants, we designed competition experiments using isogenic mutant pairs carrying targeted  
104 deletions in *oafA* and/or *gtrC*. This allowed us to study each O-antigen variant in isolation.

105

106 We first quantified selection for the genetic switch from an **O:5** to an **O:4** serotype.  
107 Competitions between *S.Tm* <sup>$\Delta oafA \Delta gtrC$</sup>  (**O:4**, O:12-locked) and *S.Tm* <sup>$\Delta gtrC$</sup>  (**O:5**, O:12-locked)  
108 were carried out in mice vaccinated against either *S.Tm* <sup>$\Delta oafA \Delta gtrC$</sup>  (**O:4**) or *S.Tm* <sup>$\Delta gtrC$</sup>  (**O:5**). IgA  
109 responses were strongly biased to recognition of the corresponding O:5 or O:4 *S.Tm* O-  
110 antigen and mediated a substantial selective advantage of expressing the alternative O-antigen  
111 variant (up to 1e7-fold by day 4, **Fig. 3A-C**). The magnitude of the selective advantage  
112 correlated tightly with the magnitude of the specific IgA response against the reactive strain  
113 (**Fig. 3B-C**). Deletion of *oafA* was fitness-neutral in naïve hosts during 4 days of infection  
114 (**Fig. 3A**). Specific IgA can therefore act as a strong evolutionary pressure selecting for  
115 mutations in genes encoding O-antigen-modifying enzymes.

116

117 We next quantified the selective advantage of phase-variation between **O:12** and **O:12-2**  
118 using strains with an *oafA*-mutant background (i.e. O:4-locked, to prevent uncontrolled O:5 to  
119 O:4 mutational changes). Mice were mock-vaccinated or vaccinated against *S.Tm* <sup>$\Delta oafA \Delta gtrC$</sup>   
120 (**O:12-locked**). Competitive infections were then carried out between *S.Tm* <sup>$\Delta oafA$</sup>  (**O:12-phase-**  
121 **variable**) and *S.Tm* <sup>$\Delta oafA \Delta gtrC$</sup>  (**O:12-locked**) strains. In line with published data, we observe a  
122 very mild fitness benefit of O:12 phase variation in naïve mice. In contrast, phase-variation  
123 was a major benefit to *S.Tm* in a subset of vaccinated animals (**Fig. 3D**). On closer  
124 examination, we observed considerable variation in the bias of IgA towards recognition of  
125 O:12 only, or of O:12 and O:12-2 with similar titres, likely due to the stochastic nature of  
126 antibody generation towards different epitopes of the O-antigen repeat. In fact, a benefit of  
127 phase-variation (i.e. a low competitiveness of the phase-locked strain) correlated with a weak  
128 anti-O:12-2 IgA response. i.e. phase-variation is beneficial whenever the phase variant is  
129 poorly bound by IgA (**Fig. 3E**). Correspondingly, O:12-phase variation, vaccine escape and  
130 inflammation were largely observed in mice where IgA bound poorly to the O:12-2 variant  
131 (**Fig 3F and G**). The mechanistic basis of this selective advantage could be confirmed by  
132 complementation of the *gtrC* gene in trans (**Fig. S7**). It is interesting to note that *gtrABC*  
133 operons are often found in temperate phage(20, 23), suggesting that the ability of *S.Tm* to  
134 quickly evade IgA mediated immunity may be further promoted by co-option of phage-  
135 encoded fitness factors (morons(33)).

136

137 Therefore IgA escapers, i.e. *S.Tm* mutants or phase variants only weakly recognized by  
138 vaccine-induced IgA, arise within 1-3 days of infection. Wherever IgA escapers dominated  
139 we observed full invasive and inflammatory disease (**Fig. S8**). Thus, both mutation and  
140 epigenetic switching processes shape the O-antigen structure of *Salmonella* and can increase  
141 the pathogen's fitness in the intestine of mice immune to specific serotypes. These changes  
142 can occur without any major loss of pathogen fitness in naïve hosts (**Fig. 3A and D**).

143

144 From these observations we hypothesized that a vaccine combining all four possible O-  
145 antigen variants (Evolutionary trap vaccine, abbreviated as PA-S.Tm<sup>ET</sup>, generated by mixing  
146 vaccines containing the **O:5,12** S.Tm <sup>$\Delta$ gtrC</sup>, **O:4,12** S.Tm <sup>$\Delta$ oafA  $\Delta$ gtrC</sup>, **O:4,12-2** S.Tm <sup>$\Delta$ oafA</sup>  
147 pgtrABC, and **O:5,12-2** S.Tm pgtrABC strains) should generate enhanced disease protection  
148 by cutting off the observed O-antigen escape pathways. Although this vaccine induced a  
149 broader antibody response (**Fig. 4A**), we observed equally good protection in both vaccinated  
150 groups (**Fig. S9**). However, closer observation revealed that PA-S.Tm<sup>ET</sup> vaccination selected  
151 for another class of O-antigen variant: mutations generating a single-repeat O-antigen(34).  
152 These can be identified by weak binding to typing antisera (**Fig. 4B**) and by gel  
153 electrophoresis of purified LPS (**Fig.4C**). Sequencing of evolved clones revealed a large  
154 deletion encompassing the *wzyB* gene, encoding the O-antigen polymerase(34) (**Fig. 4E**, **Fig.**  
155 **S10** also found in some "non-typable" S.Tm isolates from human(34)). This deletion is  
156 mediated by site-specific recombination between direct repeats flanking the *wzyB* locus. This  
157 deletion was detected in all tested S.Tm short O-antigen isolates from PA-S.Tm<sup>ET</sup> vaccinated  
158 mice across two independent experiments. We did not observe mutations in *wbaP*(34)  
159 (complete loss of O-antigen) or *opvAB*(35) (dysregulated O-antigen length). Intestinal IgA  
160 from PA-S.Tm <sup>$\Delta$ oafA</sup> vaccinated mice showed higher titres against the long O-antigen than the  
161 single-repeat O-antigen (**Fig. 4D**). This weaker binding to the very short O-antigen is  
162 consistent with lower O-antigen abundance or loss of avidity (**Fig. 4B**, **Fig. S1**).

163

164 Single infections revealed that, in comparison to isogenic wild type counterparts, *wzyB*-  
165 deficient mutants (synthetic or evolved) are significantly less efficient at colonizing the gut of  
166 streptomycin pretreated naïve mice (**Fig. 4F**), disseminating systemically (**Fig. 4G**) and  
167 triggering inflammation (**Fig. 4H**). This attenuation can be attributed to compromised outer  
168 membrane integrity(36) (**Fig S11**).

169

170 We then tested whether IgA-mediated selection could drive outgrowth of clean *wzyB* deletion  
171 mutants. Competitions between S.Tm <sup>$\Delta$ oafA  $\Delta$ gtrC</sup> (**O:4,12-locked, long O-antigen**) and S.Tm <sup>$\Delta$ oafA</sup>  
172  <sup>$\Delta$ gtrC  $\Delta$ wzyB</sup> (**O:4,12-locked, single repeat O-antigen**) mutants in the intestine of vaccinated and  
173 mock-vaccinated or antibody-deficient mice revealed a large fitness cost of the *wzyB* deletion  
174 in naive animals, as observed in earlier studies(34, 37) (**Fig. 4I**). However, in the gut of  
175 vaccinated mice, the fitness cost of decreased outer-membrane integrity in *wzyB* mutants was  
176 clearly outweighed by the benefit of avoiding O-antigen specific IgA binding (**Fig. 4I**).  
177 Vaccinated IgA<sup>-/-</sup> mice were indistinguishable from naive mice in these experiments, i.e. IgA  
178 and not any other effect of the vaccine was responsible for the phenotype. PA-S.Tm<sup>ET</sup>-elicited  
179 IgA can therefore select for mutants with a fitness cost in naïve hosts.

180

181 To demonstrate that vaccine-induced IgA, and not further genetic change in S.Tm drive this  
182 out-competition, we carried out fecal transfer experiments. Full fecal pellets from PA-S.Tm<sup>ET</sup>  
183 vaccinated mice that had been infected for 4 days with the short/long O-antigen mixture were  
184 delivered to streptomycin-treated naïve hosts. S.Tm <sup>$\Delta$ oafA  $\Delta$ gtrC  $\Delta$ wzyB</sup> (single-repeat O-antigen)  
185 dominated the population in the donor feces. However, on transfer to the naive environment  
186 the *wzyB* mutant was rapidly out-competed by the S.Tm <sup>$\Delta$ oafA  $\Delta$ gtrC</sup> (full length O-antigen) (**Fig.**  
187 **4J-L**). Thus, outgrowth in vaccinated mice is not due to compensatory mutations in the *wzyB*  
188 mutants, but to antibody-mediated selection. In real transmission settings, for example  
189 between farm animals where the intestinal niche is limited and transmission includes a period  
190 of exposure to environmental stresses, we expect these mutants to transmit very poorly.



191

192 In conclusion IgA induced by "Evolutionary Trap" vaccines can drive the outgrowth of *S.Tm*  
193 mutants producing very short O-antigens. Such mutants have a major fitness disadvantage on  
194 transmission into naive hosts, with important implications for disease spread. While the  
195 cocktail of O-antigen variants incorporated into evolutionary trap vaccines will be strain-  
196 specific, the relative ease of production and low costs of inactivated whole-cell oral vaccines  
197 suggest that this could be feasible either for pandemic strain targeting, personalized medicine  
198 or farm-specific vaccines.

199

200 Intestinal bacteria, which typically form large populations that evolve rapidly, have proven  
201 highly challenging to target with standard vaccine design: i.e. vaccines targeting a single  
202 conserved antigen. Here we suggest an alternative strategy, which turns the rapid evolution of  
203 gut bacteria from a major challenge into an advantage. Using oligovalent vaccines, we can  
204 generate a breadth of IgA responses against all fitness-neutral O-antigen modifications. These  
205 force the emergence of *S.Tm* variants with a fitness disadvantage in naïve hosts. The  
206 "Evolutionary trap" approach therefore has considerable potential as prophylaxis for diseases  
207 caused by common, increasingly antibiotic resistant, *Enterobacteriaceae* in both humans and  
208 farm animals.

## References

1. B. Liu, Y. A. Knirel, L. Feng, A. V. Perepelov, S. N. Senchenkova, P. R. Reeves, L. Wang, Structural diversity in *Salmonella* O antigens and its genetic basis. *FEMS Microbiol. Rev.* **38**, 56–89 (2014).
2. P. van der Ley, P. de Graaff, J. Tommassen, Shielding of *Escherichia coli* outer membrane proteins as receptors for bacteriophages and colicins by O-antigenic chains of lipopolysaccharide. *J. Bacteriol.* **168**, 449–451 (1986).
3. P. van der Ley, O. Kuipers, J. Tommassen, B. Lugtenberg, O-antigenic chains of lipopolysaccharide prevent binding of antibody molecules to an outer membrane pore protein in *Enterobacteriaceae*. *Microb. Pathog.* **1**, 43–9 (1986).
4. A. T. Bentley, P. E. Klebba, Effect of lipopolysaccharide structure on reactivity of antiporin monoclonal antibodies with the bacterial cell surface. *J. Bacteriol.* **170**, 1063–8 (1988).
5. K. Moor, S. Y. Wotzka, A. Toska, M. Diard, S. Hapfelmeier, E. Slack, Peracetic Acid Treatment Generates Potent Inactivated Oral Vaccines from a Broad Range of Culturable Bacterial Species. *Front. Immunol.* **7**, 34 (2016).
6. N. E. Freed, O. K. Silander, B. Stecher, A. Böhm, W.-D. Hardt, M. Ackermann, A simple screen to identify promoters conferring high levels of phenotypic noise. *PLoS Genet.* **4**, e1000307 (2008).
7. M. W. van der Woude, A. J. Bäumlner, Phase and antigenic variation in bacteria. *Clin. Microbiol. Rev.* **17**, 581–611, table of contents (2004).
8. I. D. Iankov, D. P. Petrov, I. V. Mladenov, I. H. Haralambieva, O. K. Kalev, M. S. Balabanova, I. G. Mitov, Protective efficacy of IgA monoclonal antibodies to O and H antigens in a mouse model of intranasal challenge with *Salmonella enterica* serotype Enteritidis. *Microbes Infect.* **6**, 901–910 (2004).
9. K. Moor, M. Diard, M. E. Sellin, B. Felmy, S. Y. Wotzka, A. Toska, E. Bakkeren, M. Arnoldini, F. Bansept, A. D. Co, T. Völler, A. Minola, B. Fernandez-Rodriguez, G. Agatic, S. Barbieri, L. Piccoli, C. Casiraghi, D. Corti, A. Lanzavecchia, R. R. Regoes, C. Loverdo, R. Stocker, D. R. Brumley, W.-D. Hardt, E. Slack, High-avidity IgA protects the intestine by enchainning growing bacteria. *Nature.* **544**, 498–502 (2017).
10. K. Endt, B. Stecher, S. Chaffron, E. Slack, N. Tchitchek, A. Benecke, L. Van Maele, J.-C. J.-C. Sirard, A. J. A. J. Mueller, M. Heikenwalder, A. J. A. J. Macpherson, R. Strugnell, C. von Mering, W.-D. W.-D. Hardt, The microbiota mediates pathogen

- clearance from the gut lumen after non-typhoidal salmonella diarrhea. *PLoS Pathog.* **6**, e1001097 (2010).
11. E. Valguarnera, M. F. Feldman, in *Methods in enzymology* (2017; <http://www.ncbi.nlm.nih.gov/pubmed/28935107>), vol. 597, pp. 285–310.
  12. E. Diago-Navarro, I. Calatayud-Baselga, D. Sun, C. Khairallah, I. Mann, A. Ulacia-Hernando, B. Sheridan, M. Shi, B. C. Fries, Antibody-Based Immunotherapy To Treat and Prevent Infection with Hypervirulent *Klebsiella pneumoniae*. *Clin. Vaccine Immunol.* **24** (2017), doi:10.1128/CVI.00456-16.
  13. O. Pabst, New concepts in the generation and functions of IgA. *Nat. Rev. Immunol.* **12**, 821–832 (2012).
  14. K. P. Gopalakrishna, B. R. Macadangang, M. B. Rogers, J. T. Tometich, B. A. Firek, R. Baker, J. Ji, A. H. P. Burr, C. Ma, M. Good, M. J. Morowitz, T. W. Hand, Maternal IgA protects against the development of necrotizing enterocolitis in preterm infants. *Nat. Med.* (2019), doi:10.1038/s41591-019-0480-9.
  15. WHO | Antimicrobial resistance: global report on surveillance 2014. *WHO* (2016).
  16. T. C. Darton, C. Jones, C. J. Blohmke, C. S. Waddington, L. Zhou, A. Peters, K. Haworth, R. Sie, C. A. Green, C. A. Jeppesen, M. Moore, B. A. V Thompson, T. John, R. A. Kingsley, L.-M. Yu, M. Voysey, Z. Hindle, S. Lockhart, M. B. Szein, G. Dougan, B. Angus, M. M. Levine, A. J. Pollard, Using a Human Challenge Model of Infection to Measure Vaccine Efficacy: A Randomised, Controlled Trial Comparing the Typhoid Vaccines M01ZH09 with Placebo and Ty21a. *PLoS Negl. Trop. Dis.* **10**, e0004926 (2016).
  17. B. Nagy, P. Z. Fekete, Enterotoxigenic *Escherichia coli* (EPEC) in farm animals. *Vet Res.* **30**, 259–84 (1999).
  18. S. Leach, A. Lundgren, N. Carlin, M. Löfstrand, A.-M. Svennerholm, Cross-reactivity and avidity of antibody responses induced in humans by the oral inactivated multivalent enterotoxigenic *Escherichia coli* (EPEC) vaccine ETVAX. *Vaccine.* **35**, 3966–3973 (2017).
  19. B. L. Bearson, S. M. D. Bearson, B. W. Brunelle, D. O. Bayles, I. S. Lee, J. D. Kich, Salmonella DIVA vaccine reduces disease, colonization and shedding due to virulent *S. Typhimurium* infection in swine. *J. Med. Microbiol.* **66**, 651–661 (2017).
  20. R. J. Mostowy, K. E. Holt, Diversity-Generating Machines: Genetics of Bacterial Sugar-Coating. *Trends Microbiol.* **26**, 1008–1021 (2018).
  21. D. Gerlach, Y. Guo, C. De Castro, S.-H. Kim, K. Schlatterer, F.-F. Xu, C. Pereira, P. H. Seeberger, S. Ali, J. Codée, W. Sirisarn, B. Schulte, C. Wolz, J. Larsen, A. Molinaro, B. L. Lee, G. Xia, T. Stehle, A. Peschel, Methicillin-resistant *Staphylococcus aureus* alters cell wall glycosylation to evade immunity. *Nature.* **563**, 705–709 (2018).
  22. S. E. Broadbent, M. R. Davies, M. W. van der Woude, Phase variation controls expression of *Salmonella* lipopolysaccharide modification genes by a DNA methylation-dependent mechanism. *Mol. Microbiol.* **77**, 337–53 (2010).
  23. M. R. Davies, S. E. Broadbent, S. R. Harris, N. R. Thomson, M. W. van der Woude, Horizontally acquired glycosyltransferase operons drive salmonellae lipopolysaccharide diversity. *PLoS Genet.* **9**, e1003568 (2013).
  24. B. W. Sigurskjold, E. Altman, D. R. Bundle, Sensitive titration microcalorimetric study of the binding of *Salmonella* O-antigenic oligosaccharides by a monoclonal antibody. *Eur. J. Biochem.* **197**, 239–246 (1991).
  25. D. A. Brummell, V. P. Sharma, N. N. Anand, D. Bilous, G. Dubuc, J. Michniewicz, C. R. MacKenzie, J. Sadowska, B. W. Sigurskjold, B. Sinnott, Probing the combining site of an anti-carbohydrate antibody by saturation-mutagenesis: role of the heavy-chain CDR3 residues. *Biochemistry.* **32**, 1180–7 (1993).
  26. M. Yang, R. Simon, A. D. MacKerell, Jr., Conformational Preference of Serogroup B *Salmonella* O Polysaccharide in Presence and Absence of the Monoclonal Antibody Se155-4. *J. Phys. Chem. B.* **121**, 3412–3423 (2017).
  27. K. Ilg, G. Zandomenighi, G. Rugarabamu, B. H. Meier, M. Aebi, HR-MAS NMR



- reveals a pH-dependent LPS alteration by de-O-acetylation at abequose in the O-antigen of *Salmonella enterica* serovar Typhimurium. *Carbohydr. Res.* **382**, 58–64 (2013).
28. E. Hauser, E. Junker, R. Helmuth, B. Malorny, Different mutations in the oafA gene lead to loss of O5-antigen expression in *Salmonella enterica* serovar Typhimurium. *J. Appl. Microbiol.* **110**, 248–53 (2011).
  29. Y. Nakai, A. Ito, Y. Ogawa, S. D. Aribam, M. Elsheimer-Matulova, K. Shiraiwa, S. M. B. Kisaka, H. Hikono, S. Nishikawa, M. Akiba, K. Kawahara, Y. Shimoji, M. Eguchi, Determination of O:4 antigen-antibody affinity level in O:5 antigen positive and negative variants of *Salmonella enterica* serovar Typhimurium. *FEMS Microbiol. Lett.* **364** (2017), doi:10.1093/femsle/fnx062.
  30. M. Bichara, J. Wagner, I. B. Lambert, Mechanisms of tandem repeat instability in bacteria. *Mutat. Res. Mol. Mech. Mutagen.* **598**, 144–163 (2006).
  31. L. M. Bogomolnaya, C. A. Santiviago, H.-J. Yang, A. J. Baumler, H. L. Andrews-Polymeris, “Form variation” of the O12 antigen is critical for persistence of *Salmonella* Typhimurium in the murine intestine. *Mol. Microbiol.* **70**, 1105–19 (2008).
  32. E. Kintz, C. Heiss, I. Black, N. Donohue, N. Brown, M. R. Davies, P. Azadi, S. Baker, P. M. Kaye, M. van der Woude, *Salmonella enterica* Serovar Typhi Lipopolysaccharide O-Antigen Modification Impact on Serum Resistance and Antibody Recognition. *Infect. Immun.* **85** (2017), doi:10.1128/IAI.01021-16.
  33. H. Brussow, C. Canchaya, W.-D. Hardt, Phages and the Evolution of Bacterial Pathogens: from Genomic Rearrangements to Lysogenic Conversion. *Microbiol. Mol. Biol. Rev.* **68**, 560–602 (2004).
  34. I. Szabo, M. Grafe, N. Kemper, E. Junker, B. Malorny, Genetic basis for loss of immuno-reactive O-chain in *Salmonella enterica* serovar Enteritidis veterinary isolates. *Vet. Microbiol.* **204**, 165–173 (2017).
  35. I. Cota, M. A. Sánchez-Romero, S. B. Hernández, M. G. Pucciarelli, F. García-Del Portillo, J. Casadesús, Epigenetic Control of *Salmonella enterica* O-Antigen Chain Length: A Tradeoff between Virulence and Bacteriophage Resistance. *PLoS Genet.* **11**, e1005667 (2015).
  36. E. R. Rojas, G. Billings, P. D. Odermatt, G. K. Auer, L. Zhu, A. Miguel, F. Chang, D. B. Weibel, J. A. Theriot, K. C. Huang, The outer membrane is an essential load-bearing element in Gram-negative bacteria. *Nature.* **559**, 617–621 (2018).
  37. G. L. Murray, S. R. Attridge, R. Morona, Altering the length of the lipopolysaccharide O antigen has an impact on the interaction of *Salmonella enterica* serovar Typhimurium with macrophages and complement. *J. Bacteriol.* **188**, 2735–9 (2006).
  38. A. Varki, R. D. Cummings, M. Aebi, N. H. Packer, P. H. Seeberger, J. D. Esko, P. Stanley, G. Hart, A. Darvill, T. Kinoshita, J. J. Prestegard, R. L. Schnaar, H. H. Freeze, J. D. Marth, C. R. Bertozzi, M. E. Etzler, M. Frank, J. F. Vliegenthart, T. Lütteke, S. Perez, E. Bolton, P. Rudd, J. Paulson, M. Kanehisa, P. Toukach, K. F. Aoki-Kinoshita, A. Dell, H. Narimatsu, W. York, N. Taniguchi, S. Kornfeld, Symbol Nomenclature for Graphical Representations of Glycans. *Glycobiology.* **25**, 1323–1324 (2015).
  39. G. R. Harriman, M. Bogue, P. Rogers, M. Finegold, S. Pacheco, A. Bradley, Y. Zhang, I. N. Mbawuiké, Targeted deletion of the IgA constant region in mice leads to IgA deficiency with alterations in expression of other Ig isotypes. *J. Immunol.* **162**, 2521–9 (1999).
  40. H. Gu, Y. R. Zou, K. Rajewsky, Independent control of immunoglobulin switch recombination at individual switch regions evidenced through Cre-loxP-mediated gene targeting. *Cell.* **73**, 1155–64 (1993).
  41. P. Mombaerts, J. Iacomini, R. S. Johnson, K. Herrup, S. Tonegawa, V. E. Papaioannou, RAG-1-deficient mice have no mature B and T lymphocytes. *Cell.* **68**, 869–77 (1992).
  42. K. A. Datsenko, B. L. Wanner, One-step inactivation of chromosomal genes in *Escherichia coli* K-12 using PCR products. *Proc. Natl. Acad. Sci.* **97**, 6640–6645

- (2000).
43. N. L. Sternberg, R. Maurer, Bacteriophage-mediated generalized transduction in *Escherichia coli* and *Salmonella typhimurium*. *Methods Enzymol.* **204**, 18–43 (1991).
  44. B. Stecher, S. Hapfelmeier, C. Muller, M. Kremer, T. Stallmach, W.-D. Hardt, Flagella and Chemotaxis Are Required for Efficient Induction of *Salmonella enterica* Serovar Typhimurium Colitis in Streptomycin-Pretreated Mice. *Infect. Immun.* **72**, 4138–4150 (2004).
  45. A. M. Bolger, M. Lohse, B. Usadel, Trimmomatic: a flexible trimmer for Illumina sequence data. *Bioinformatics.* **30**, 2114–2120 (2014).
  46. H. Li, R. Durbin, Fast and accurate short read alignment with Burrows-Wheeler transform. *Bioinformatics.* **25**, 1754–1760 (2009).
  47. B. J. Walker, T. Abeel, T. Shea, M. Priest, A. Abouelliel, S. Sakthikumar, C. A. Cuomo, Q. Zeng, J. Wortman, S. K. Young, A. M. Earl, Pilon: an integrated tool for comprehensive microbial variant detection and genome assembly improvement. *PLoS One.* **9**, e112963 (2014).
  48. P. Cingolani, A. Platts, L. L. Wang, M. Coon, T. Nguyen, L. Wang, S. J. Land, X. Lu, D. M. Ruden, A program for annotating and predicting the effects of single nucleotide polymorphisms, SnpEff: SNPs in the genome of *Drosophila melanogaster* strain w1118; iso-2; iso-3. *Fly (Austin).* **6**, 80–92 (2012).
  49. K. Moor, S. Y. Wotzka, A. Toska, M. Diard, S. Hapfelmeier, E. Slack, Peracetic Acid Treatment Generates Potent Inactivated Oral Vaccines from a Broad Range of Culturable Bacterial Species. *Front. Immunol.* **7** (2016), doi:10.3389/fimmu.2016.00034.
  50. M. Barthel, S. Hapfelmeier, L. Quintanilla-Martínez, M. Kremer, M. Rohde, M. Hogardt, K. Pfeffer, H. Rüssmann, W.-D. Hardt, Pretreatment of mice with streptomycin provides a *Salmonella enterica* serovar Typhimurium colitis model that allows analysis of both pathogen and host. *Infect. Immun.* **71**, 2839–58 (2003).
  51. K. Moor, J. Fadlallah, A. Toska, D. Sterlin, M. L. Balmer, A. J. Macpherson, G. Gorochoy, M. Larsen, E. Slack, Analysis of bacterial-surface-specific antibodies in body fluids using bacterial flow cytometry. *Nat. Protoc.* **11**, 1531–1553 (2016).
  52. M. Arnoldini, I. A. Vizcarra, R. Peña-Miller, N. Stocker, M. Diard, V. Vogel, R. E. Beardmore, W.-D. Hardt, M. Ackermann, Bistable expression of virulence genes in salmonella leads to the formation of an antibiotic-tolerant subpopulation. *PLoS Biol.* **12**, e1001928 (2014).
  53. S. van Vliet, A. Dal Co, A. R. Winkler, S. Spriewald, B. Stecher, M. Ackermann, Spatially Correlated Gene Expression in Bacterial Groups: The Role of Lineage History, Spatial Gradients, and Cell-Cell Interactions. *Cell Syst.* **6**, 496-507.e6 (2018).
  54. O. Westphal, K. Jann, Bacterial Lipopolysaccharides Extraction with Phenol-Water and Further Applications of the Procedure. *Methods Carbohydr. Chem.* **5**, 83–91 (1965).
  55. T. Steffens, K. Duda, B. Lindner, F.-J. Vorhölter, H. Bednarz, K. Niehaus, O. Holst, The lipopolysaccharide of the crop pathogen *Xanthomonas translucens* pv. *translucens*: chemical characterization and determination of signaling events in plant cells. *Glycobiology.* **27**, 264–274 (2017).
  56. S. Ardissonne, P. Redder, G. Russo, A. Frandi, C. Fumeaux, A. Patrignani, R. Schlapbach, L. Falquet, P. H. Viollier, Cell Cycle Constraints and Environmental Control of Local DNA Hypomethylation in  $\alpha$ -Proteobacteria. *PLoS Genet.* **12**, e1006499 (2016).
  57. H. Li, A statistical framework for SNP calling, mutation discovery, association mapping and population genetical parameter estimation from sequencing data. *Bioinformatics.* **27**, 2987–93 (2011).
  58. D. W. Barnett, E. K. Garrison, A. R. Quinlan, M. P. Strömberg, G. T. Marth, BamTools: a C++ API and toolkit for analyzing and managing BAM files. *Bioinformatics.* **27**, 1691–2 (2011).
  59. A. R. Quinlan, I. M. Hall, BEDTools: a flexible suite of utilities for comparing

- genomic features. *Bioinformatics*. **26**, 841–2 (2010).
60. P. J. Kersey, J. E. Allen, I. Armean, S. Boddu, B. J. Bolt, D. Carvalho-Silva, M. Christensen, P. Davis, L. J. Falin, C. Grabmueller, J. Humphrey, A. Kerhornou, J. Khobova, N. K. Aranganathan, N. Langridge, E. Lowy, M. D. McDowall, U. Maheswari, M. Nuhn, C. K. Ong, B. Overduin, M. Paulini, H. Pedro, E. Perry, G. Spudich, E. Tapanari, B. Walts, G. Williams, M. Tello–Ruiz, J. Stein, S. Wei, D. Ware, D. M. Bolser, K. L. Howe, E. Kulesha, D. Lawson, G. Maslen, D. M. Staines, Ensembl Genomes 2016: more genomes, more complexity. *Nucleic Acids Res.* **44**, D574–D580 (2016).
  61. M. RStudio, Inc., Boston, RStudio: Integrated Development for R, (available at <https://www.rstudio.com/>).
  62. R: A Language and Environment for Statistical Computing. R Foundation for Statistical Computing, (available at <https://www.r-project.org/about.html>).
  63. M. I. Love, W. Huber, S. Anders, Moderated estimation of fold change and dispersion for RNA-seq data with DESeq2. *Genome Biol.* **15**, 550 (2014).
  64. H. Yamashita, A. Taoka, T. Uchihashi, T. Asano, T. Ando, Y. Fukumori, Single-Molecule Imaging on Living Bacterial Cell Surface by High-Speed AFM. *J. Mol. Biol.* **422**, 300–309 (2012).
  65. M. Hoffmann, T. Muruvanda, M. W. Allard, J. Korlach, R. J. Roberts, R. Timme, J. Payne, P. F. McDermott, P. Evans, J. Meng, E. W. Brown, S. Zhao, Complete Genome Sequence of a Multidrug-Resistant *Salmonella enterica* Serovar Typhimurium var. 5- Strain Isolated from Chicken Breast. *Genome Announc.* **1** (2013), doi:10.1128/genomeA.01068-13.
  66. C. Silva, E. Calva, J. L. Puente, M. B. Zaidi, P. Vinuesa, Complete Genome Sequence of *Salmonella enterica* Serovar Typhimurium Strain SO2 (Sequence Type 302) Isolated from an Asymptomatic Child in Mexico. *Genome Announc.* **4** (2016), doi:10.1128/genomeA.00253-16.
  67. Y. Hong, M. A. Liu, P. R. Reeves, Progress in Our Understanding of Wzx Flippase for Translocation of Bacterial Membrane Lipid-Linked Oligosaccharide. *J. Bacteriol.* **200**, e00154-17 (2018).
  68. S. K. Hoiseth, B. A. D. Stocker, Aromatic-dependent *Salmonella typhimurium* are non-virulent and effective as live vaccines. *Nature*. **291**, 238–239 (1981).
  69. S. Hapfelmeier, B. Stecher, M. Barthel, M. Kremer, A. J. Müller, M. Heikenwalder, T. Stallmach, M. Hensel, K. Pfeffer, S. Akira, W.-D. Hardt, The *Salmonella* Pathogenicity Island (SPI)-2 and SPI-1 Type III Secretion Systems Allow *Salmonella* Serovar *typhimurium* to Trigger Colitis via MyD88-Dependent and MyD88-Independent Mechanisms. *J. Immunol.* **174**, 1675–1685 (2005).

### **Acknowledgements**

OH acknowledges Heiko Käbner for recording NMR spectra, Regina Engel for GLC-MS, and Katharina Jakob and Sylvia Düpow for technical support. We want to thank Magdalena Schneider, Christine Kiessling, Elisabeth Schultheiss, Rosa-Maria Vesco and Clarisse Straub for the DNA extraction, library preparations and sequencing of the bacterial isolates. MD acknowledges Delphine Cornillet for serum resistance measurements.

### **Funding**

MD is supported by a SNF professorship (PP00PP\_176954). ES acknowledges the support of the Swiss National Science Foundation (40B2-0\_180953, 310030\_185128) and Gebert Rüt Microbials (GR073\_17). BMS acknowledges the support of R01 AI041239/AI/NIAID NIH HHS/United States. WDH acknowledges support by grants from the Swiss National Science Foundation (SNF; 310030B-173338), the Promedica Foundation, Chur and the Helmut Horten Foundation. EB is supported by a Boehringer Ingelheim Fonds PhD fellowship. BM acknowledges support by the Swiss National Science Foundation (200020\_159707).

### **Author contributions**

MD, WDH and ES designed the project and wrote the paper. MD and ES designed and carried out experiments. MvdW, BHM, RM contributed to experimental design / data interpretation. EB, DH, VL FB, KSM, AH, JA, PV, LV, DW, FB, AE, GZ, OH, MA carried out analyses shown in Fig1-4 and S1-S9. ND produced strains 891 and 931. LP, AL and BMS generated novel antibody reagents. All authors critically reviewed the manuscript.

### **Conflict of Interest**

The authors declare that Evolutionary Trap Vaccines are covered by European patent application EP19177251.

### **Data and materials availability**

All data and materials are in the manuscript or will be provided on request to the corresponding authors.

### **List of Supplementary Materials:**

- Materials and Methods
- Supplementary Figures S1-11
- Supplementary Table S1-3
- Supplementary Movies 1 and 2

## Figures 1-4

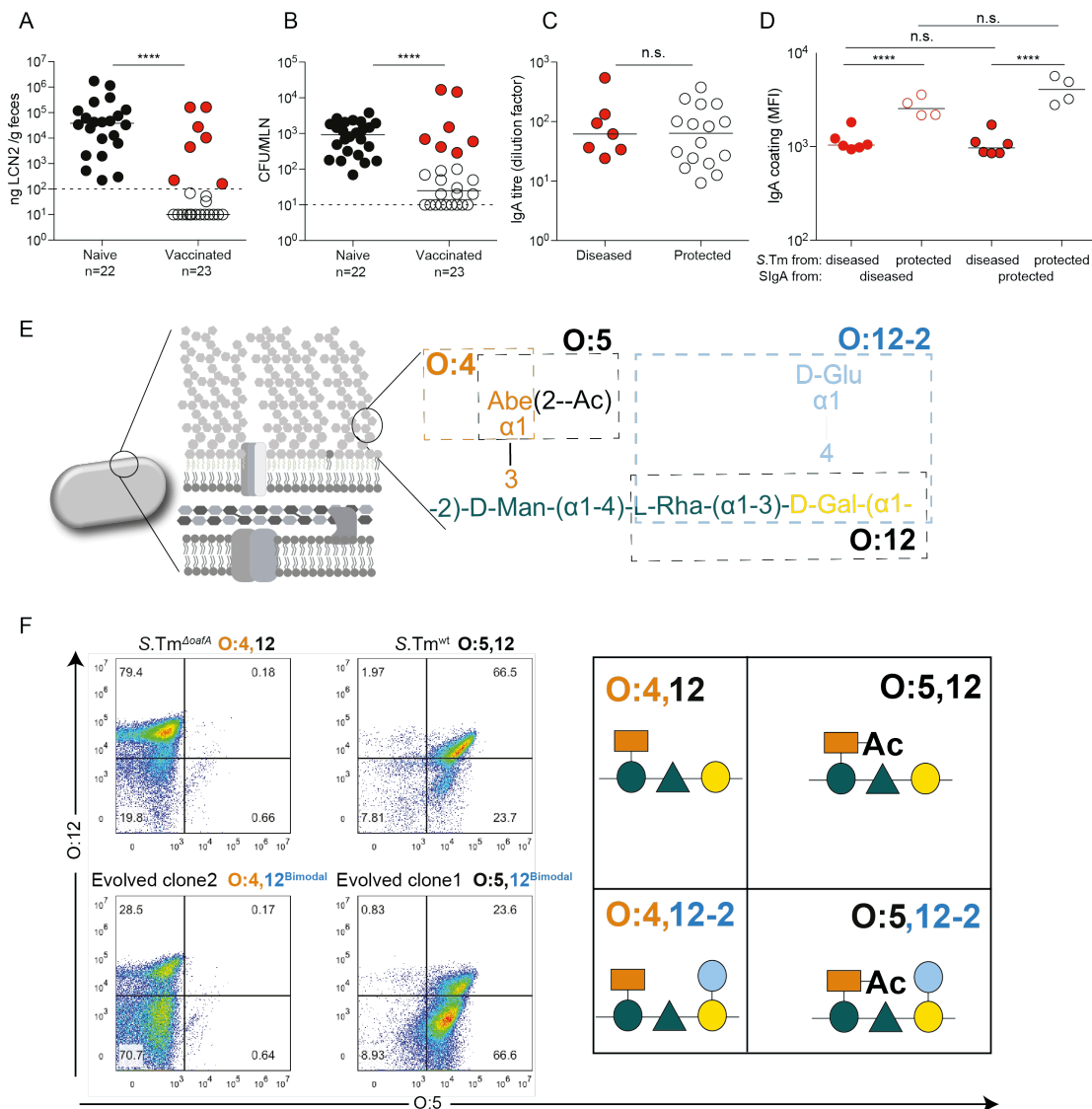


**Figure 1: IgA-escape by O-antigen modification:** A-C: Naive or PA-*S.Tm*-vaccinated (Vaccinated) mice were streptomycin-pretreated, infected ( $10^5$  *S.Tm*<sup>wt</sup> Colony forming units (CFU) per os) and analyzed 18 h later. **A.** Fecal Lipocalin 2 (LCN2) to quantify intestinal inflammation, **B.** Pathogen loads (CFU) in mesenteric lymph nodes (MLN), **C.** Intestinal IgA titres against *S.Tm*<sup>wt</sup> determined by flow cytometry, for vaccinated mice with LCN2 values below (open symbols, protected) and above (filled symbols, diseased) 100ng/g.  $p=0.61$  by Mann Whitney U test. **D.** Mice vaccinated and infected as in A-C. Ability of intestinal lavage IgA from diseased vaccinated mouse (red borders) or a protected vaccinated mouse (black borders) to recognize *S.Tm* clones re-isolated from the feces of the diseased mouse (red filled circles) or protected mouse (open circles) at day 3 post-infection. 2-way ANOVA with Bonferroni post-tests. **E.** Schematic of the O-antigen of *S.Tm* (O:5,12), and its common variants (O:4,12<sub>2</sub>), coloured to correspond to the "Symbol Nomenclature for Glycans". **F.** Overnight cultures of the indicated *S.Tm* strains and evolved clones arising during infections with *S.Tm*<sup>wt</sup> were stained with anti-O:5 and anti-O:12 antibodies, followed by fluorescent secondary reagents. Representative flow cytometry analyses of the different O-antigen types, and the "Symbol Nomenclature for Graphical Representations of Glycans"(38) representation of the O-antigen repeat structure present on *S.Tm* in each quadrant of the flow cytometry plots.



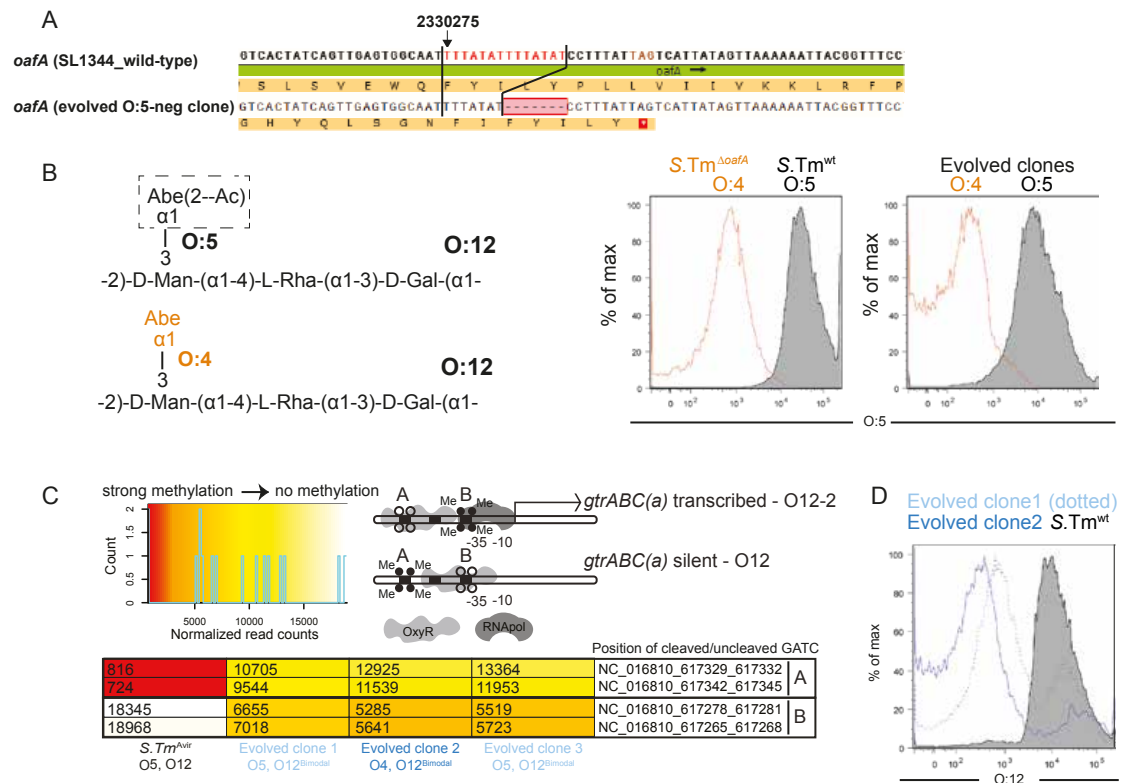


**Figure 2: Genetic and epigenetic changes underlie escape:** **A.** Alignment of the *oafA* sequence from wild type (SL1344\_RS11465) and an example O:5-negative evolved clone showing the 7bp contraction (all four re-sequenced O:5-negative strains showed the same deletion). **B.** Flow cytometry staining of *S.Tm*, *S.Tm*<sup>Δ*oafA*</sup>, and two evolved clones differing in O:5 status with anti-O:5 typing sera. **C.** Methylation status of the *gtrABC* promoter region in *S.Tm*, and three O:12<sup>Bimodal</sup> evolved clones determined by REC-seq. Heat-scale for normalized read-counts, schematic diagram of promoter methylation associated with ON and OFF phenotypes, and normalized methylation read counts for the indicated strains. **D.** Binding of an O:12-specific monoclonal antibody to *S.Tm* and O:12<sup>Bimodal</sup> evolved clones, determined by bacterial flow cytometry.

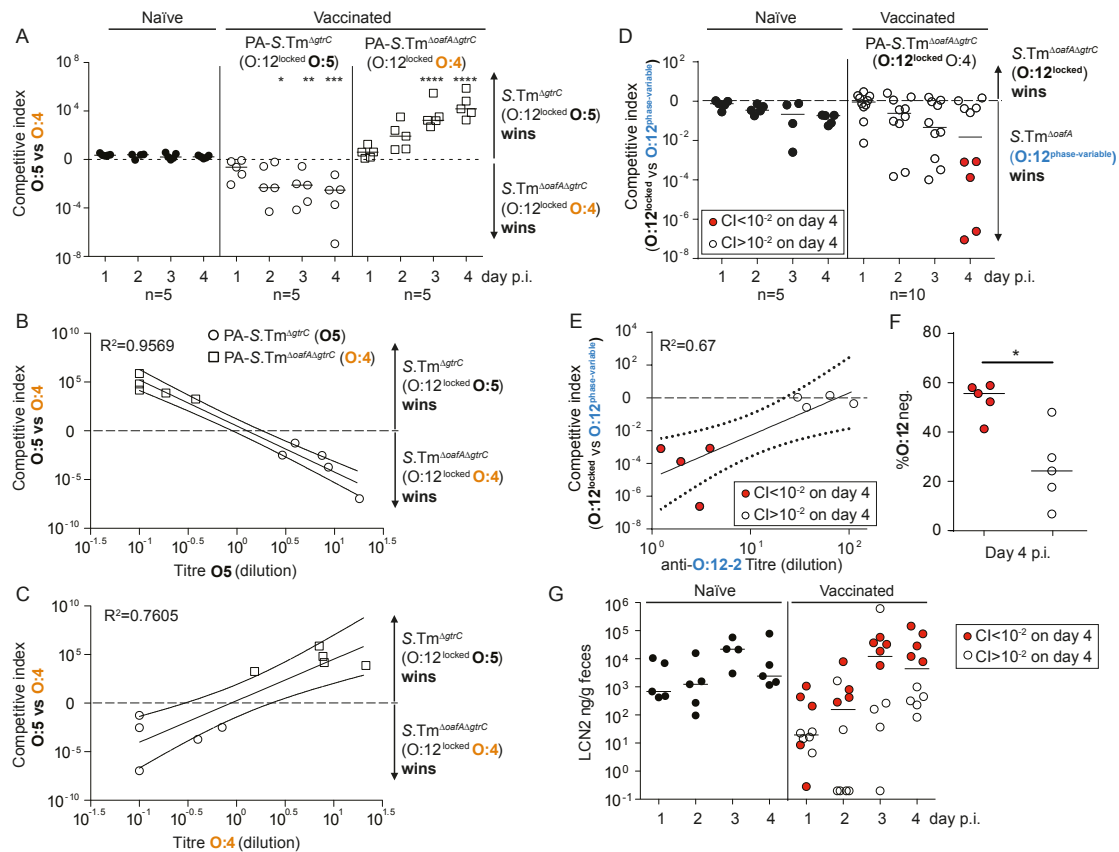


**Figure 3: O-antigen modification confers a selective advantage in the presence of vaccine-induced IgA: A-C.** Naive (closed circles), PA-*S.Tm* <sup>$\Delta$ grC</sup>-vaccinated (O:5-vaccinated, open circles) and PA-*S.Tm* <sup>$\Delta$ grC  $\Delta$ oafA</sup>-vaccinated (O:4-vaccinated, open squares) mice were streptomycin-pretreated, infected (10<sup>5</sup> CFU, 1:1 ratio of *S.Tm* <sup>$\Delta$ grC</sup> and *S.Tm* <sup>$\Delta$ grC  $\Delta$ oafA</sup> per os). **A.** Competitive index (CFU *S.Tm* <sup>$\Delta$ grC</sup>/CFU *S.Tm* <sup>$\Delta$ grC  $\Delta$ oafA</sup>) in feces at the indicated time-points. 2-way ANOVA with Bonferroni post-tests on log-normalized values, compared to naive mice. \*p<0.05, \*\*p<0.01, \*\*\*p<0.001, \*\*\*\*p<0.0001. **B and C.** Correlation of the competitive index with the O:5-specific (**B**) and O:4-specific (**C**) intestinal IgA titre, r<sup>2</sup> values of the linear regression of log-normalized values. Open circles: Intestinal IgA from O:5-vaccinated mice, Open squares: Intestinal IgA from O:4-vaccinated mice. Lines indicate the best fit with 95% confidence interval **D-G.** Naive (closed circles) or PA-*S.Tm* <sup>$\Delta$ oafA  $\Delta$ grC</sup>-vaccinated (O:4/O:12-vaccinated, open circles and red circles) mice were streptomycin-pretreated and infected (10<sup>5</sup> CFU, 1:1 ratio of *S.Tm* <sup>$\Delta$ oafA</sup> (O:12-2 switching) and *S.Tm* <sup>$\Delta$ oafA  $\Delta$ grC</sup> (O:12-locked) per os). **D.** Competitive index (CFU *S.Tm* <sup>$\Delta$ oafA  $\Delta$ grC</sup> /CFU *S.Tm* <sup>$\Delta$ oafA</sup>) in feces at the indicated time-points. Red circles indicate vaccinated mice with a competitive index of below 10<sup>-2</sup> and are used to identify these animals in panels **D-G.** Effect of vaccination is not significant by 2-way ANOVA considering vaccination over time. **E.** Correlation of the competitive index on day 4 with the intestinal IgA titre against an O:12-2-locked *S.Tm* *pgtrABC* variant (linear regression of log-normalized values, lines indicate the best fit with 95% confidence interval). **F.** Enrichment cultures of the fecal *S.Tm* <sup>$\Delta$ oafA</sup> population at day 4 were stained for O:12/O:4 and the fraction of O:12-negative *S.Tm* quantified by flow cytometry. **G.** Intestinal inflammation quantified by Fecal Lipocalin 2 (LCN2).

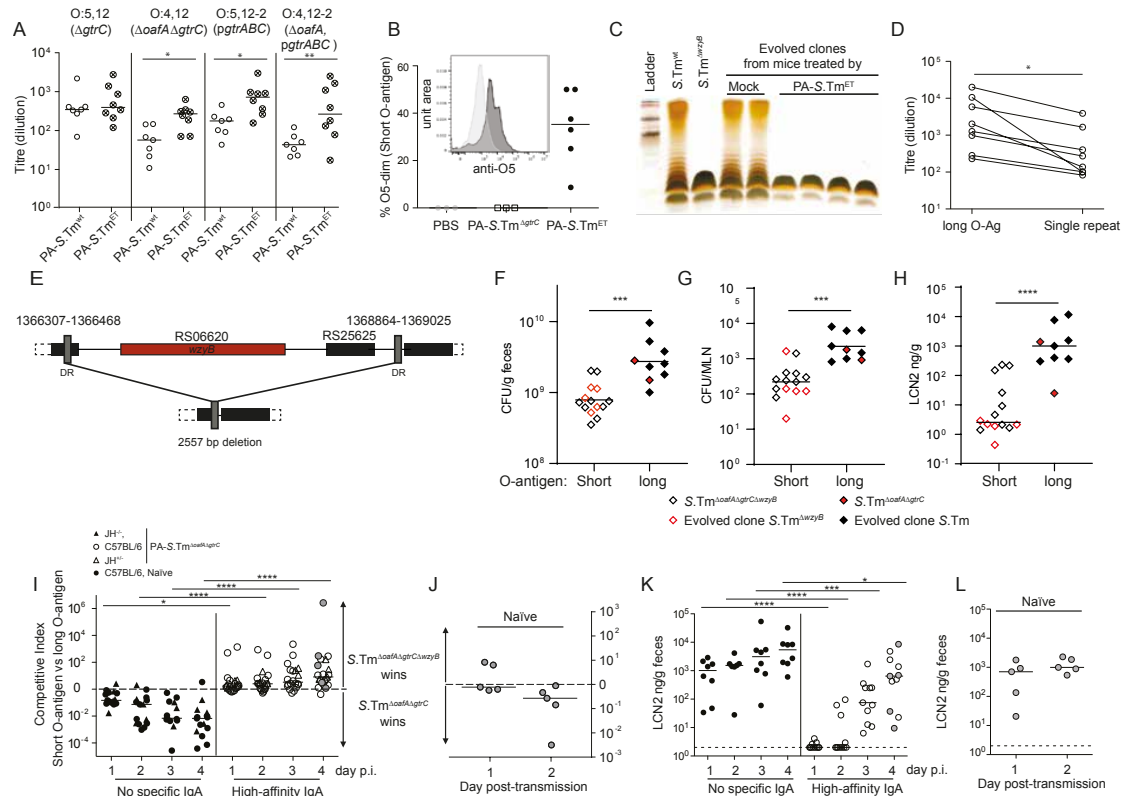


**Figure 4: Vaccines combining fitness-neutral glycan variants set an evolutionary trap for *S.Tm*, selecting for strains with a single-repeat O-antigen:** **A and B.** *S.Tm* clones re-isolated from the feces of mice vaccinated with PBS only, PA-*S.Tm*<sup>ΔgrC</sup> or PA-*S.Tm*<sup>ET</sup> (combined PA-*S.Tm*<sup>ΔgrC</sup>, PA-*S.Tm*<sup>ΔoafA ΔgrC</sup>, PA-*S.Tm* *pgtrABC*, and PA-*S.Tm*<sup>ΔoafA pgtrABC</sup>). **A.** Intestinal IgA titre, determined by bacterial flow cytometry against *S.Tm*<sup>ΔgrC</sup> (O:5,12), *S.Tm*<sup>ΔoafA ΔgrC</sup> (O:4,12), *S.Tm*<sup>ΔgrC pgtrABC</sup> (O:5, 12-2) and *S.Tm*<sup>ΔoafA ΔgrC pgtrABC</sup> (O:4,12-2). **B.** Fraction of clones with weak anti-sera staining, as determined by flow cytometry, indicative of O-antigen shortening. One point represents one mouse. **C.** Silver-stained gel of LPS from control and evolved *S.Tm* strains from control and PA-*S.Tm*<sup>ET</sup> vaccinated mice, showing short LPS in clones isolated from vaccinated PA-*S.Tm*<sup>ET</sup> mice. **D.** Intestinal IgA titre from PA-*S.Tm*<sup>ΔoafA ΔgrC</sup>-vaccinated mice specific for *S.Tm*<sup>ΔoafA ΔgrC</sup> (long O-antigen) and *S.Tm*<sup>ΔoafA ΔgrC ΔwzyB</sup> (short O-antigen). **E.** Resequencing of strains with short O-antigen reveals a large genomic deletion between inverted repeats, covering the *wzyB* gene (O-antigen polymerase) n=5 clones sequenced. **F, G, H,** Single 24h infections in streptomycin pretreated naïve mice. Evolved and synthetic *wzyB* mutants have reduced ability to colonize the gut (**F**, CFU/g feces) and to spread systemically (**G**, CFU per mesenteric lymph node (MLN)). This translates into diminished propensity to trigger intestinal inflammation in comparison to *wzyB* wild type strains (**H**, fecal Lipocalin 2 (LCN2)). **I.** Mock-vaccinated wild type (C57BL/6, mock), PA-*S.Tm*<sup>ΔoafA ΔgrC</sup>-vaccinated JH<sup>-/-</sup> mice (JH<sup>-/-</sup>, Vacc), PA-*S.Tm*<sup>ΔoafA ΔgrC</sup>-vaccinated wild type (C57BL/6, Vacc) and PA-*S.Tm*<sup>ΔoafA ΔgrC</sup>-vaccinated JH<sup>+/-</sup> littermate controls (JH<sup>+/-</sup>, Vacc) mice were streptomycin pre-treated and infected with 10<sup>5</sup> CFU of a 1:1 ratio *S.Tm*<sup>ΔoafA ΔgrC ΔwzyB</sup> and *S.Tm*<sup>ΔoafA ΔgrC</sup>. i.e. serotype-locked, short and long O-antigen-producing strains. Competitive index of *S.Tm* in feces on the indicated days. **J.** Feces from the indicated mice (grey-filled circles) from panel **I** were transferred into streptomycin-pretreated naïve mice (one fecal pellet per mouse) and competitive index in feces calculated to day 2 post-infection. **K and L.** Fecal Lipocalin 2 (LCN2) corresponding to panels **I** and **J** respectively. **A, I, K.** 2-way ANOVA on log-Normalized data. Bonferroni post-test statistics are shown. In panel **I**, competitive index in vaccinated mice is significantly higher than 1 at all time-points by Wilcoxon signed rank tests. **D, F, G, H:** Mann-Whitney U 2-tailed tests.

## 1 **Supplementary Materials**

### 2 **Materials and methods:**

3

#### 4 **Ethics statement**

5 All animal experiments were approved by the legal authorities (licenses 223/2010, 222/2013  
6 and 193/2016; Kantonales Veterinäramt Zürich, Switzerland) and performed according to the  
7 legal and ethical requirements.

8

#### 9 **Mice**

10 Unless otherwise stated, all experiments used SOPF C57BL/6 mice. 129S1/SvImJ, IgA<sup>-/-</sup>  
11 [(39)<sup>1</sup>], J<sub>H</sub><sup>-/-</sup> [(40)<sup>1</sup>], Rag1<sup>-/-</sup> [(41)<sup>1</sup>] (all C57BL/6 background) were re-derived into a specific  
12 opportunistic pathogen-free (SOPF) foster colony to normalize the microbiota and bred under  
13 full barrier conditions in individually ventilated cages in the ETH Phenomics center (EPIC,  
14 RCHCI), ETH Zürich. Low complex microbiota (LCM) mice (C57BL/6) are ex-germfree  
15 mice, which were colonized with a naturally diversified Altered Schaedler flora in 2007(10)  
16 and were bred in individually ventilated cages or flexible-film isolators at this facility.  
17 Vaccinations were started between 5 and 6 weeks of age, and males and females were  
18 randomized between groups to obtain identical ratios wherever possible. As strong  
19 phenotypes were expected, we adhered to standard practice of analysing at least 5 mice per  
20 group. Researchers were not blinded to group allocation.

21

#### 22 **Strains and plasmids**

23 All strains and plasmids used in this study are listed **Table S1**.

24 For cultivation of bacteria, we used lysogeny broth (LB) containing appropriate antibiotics  
25 (i.e., 50 µg/ml streptomycin (AppliChem); 6 µg/ml chloramphenicol (AppliChem); 50 µg/ml  
26 kanamycin (AppliChem); 100 µg/ml ampicillin (AppliChem)). Dilutions were prepared in  
27 Phosphate Buffer Saline (PBS, Difco)

28 In-frame deletion mutants (e.g. *gtrC::cat*) were performed by  $\lambda$  red recombination as  
29 described in(42). When needed, antibiotic resistance cassettes were removed using the  
30 temperature-inducible FLP recombinase encoded on pCP20(42). Mutations coupled with  
31 antibiotic resistance cassettes were transferred into the relevant genetic background by  
32 generalized transduction with bacteriophage P22 HT105/1 *int-201*(43). Primers used for  
33 genetic manipulations and verifications of the constructions are listed **Table S2**. Deletions of  
34 *gtrA* and *gtrC* originated from in-frame deletions made in S.Tm 14028S, kind gifts from Prof.  
35 Michael McClelland (University of California, Irvine), and were transduced into the SB300  
36 genetic background.

37

38 The *gtrABC* operon (STM0557-0559) was cloned into the pSC101 derivative plasmid  
39 pM965(44). The operon *gtrABC* was amplified from the chromosome of SB300 using the  
40 Phusion Polymerase (ThermoFisher Scientific) and primers listed **Table S2**. The PCR product  
41 and pM965 were digested with PstI-HF and EcoRV-HF (NEB) before kit purification (SV  
42 Gel and PCR Clean up System, Promega) and ligation in presence of T4 ligase (NEB)  
43 following manufacturer recommendations. The ligation product was transferred by electro-  
44 transformation in competent SB300 cells.

45

#### 46 **Targeted sequencing**

47 Targeted re-sequencing by the Sanger method (Microsynth AG) was performed on kit  
48 purified PCR products (Promega) from chromosomal DNA or expression vector templates  
49 using pre-mixed sequencing primers listed **Table S2**.

50

#### 51 **Whole-genome re-sequencing of O:12<sup>Bimodal</sup> isolates**

52 The genomes of *S.Tm* and evolved derivatives were fully sequenced by the Miseq system  
53 (2x300bp reads, Illumina, San Diego, CA) operated at the Functional Genomic Center in  
54 Zurich. The sequence of *S.Tm* SL1344 (NC\_016810.1) was used as reference. Quality check,  
55 reads trimming, alignments, SNPs and indels calling were performed using the bioinformatics  
56 software CLC Workbench (Qiagen).

57

#### 58 **Whole-genome sequencing of *S.Tm* isolates from "Evolutionary trap" vaccinated mice 59 and variant calling.**

60 Nextera XT libraries were prepared for each of the samples. The barcoded libraries were  
61 pooled into equimolar concentrations following manufacturer's guidelines (Illumina, San  
62 Diego, CA) using the Mid-Output Kit for paired-end sequencing (2×150 bp) on an Illumina  
63 NextSeq500 sequencing platform. Raw data (mean virtual coverage 361x) was demultiplexed  
64 and subsequently clipped of adapters using Trimmomatic v0.38 with default parameters(45).  
65 Quality control passing read-pairs were aligned against reference genome/plasmids  
66 (Accession numbers: NC\_016810.1, NC\_017718.1, NC\_017719.1, NC\_017720.1) with bwa  
67 v0.7.17(46). Genomic variant were called using Pilon v1.23(47). with the following  
68 parameters: (i) minimum coverage 10x; (ii) minimum quality score = 20; (iii) minimum read  
69 mapping quality = 10. SnpEff v4.3 was used to annotate variants according to NCBI and  
70 predict their effect on genes(48).

71

#### 72 **PA-*S.Tm* vaccinations**

73 Peracetic acid killed vaccines were produced as previously described(49). Briefly, bacteria  
74 were grown overnight to late stationary phase, harvested by centrifugation and re-suspended  
75 to a density of 10<sup>9</sup>-10<sup>10</sup> per ml in sterile PBS. Peracetic acid (Sigma-Aldrich) was added to a  
76 final concentration of 0.4% v/v. The suspension was mixed thoroughly and incubated for 60  
77 min at room temperature. Bacteria were washed once in 40 ml of sterile 10x PBS and  
78 subsequently three times in 50 ml sterile 1x PBS. The final pellet was re-suspended to yield a  
79 density of 10<sup>11</sup> particles per ml in sterile PBS (determined by OD600) and stored at 4°C for  
80 up to three weeks. As a quality control, each batch of vaccine was tested before use by  
81 inoculating 100 µl of the killed vaccine (one vaccine dose) into 300 ml LB and incubating  
82 over night at 37 °C with aeration. Vaccine lots were released for use only when a negative  
83 enrichment culture had been confirmed.

84

#### 85 **Non-typhoidal *Salmonella* challenge infections**

86 Infections were carried out as described(50). In order to allow reproducible gut colonization,  
87 8-12 week-old C57Bl/6 mice, naïve or vaccinated, were orally pretreated 24 h before  
88 infection with 25 mg streptomycin. Strains were cultivated overnight separately in LB  
89 containing the appropriate antibiotics. Subcultures were prepared before infections by diluting  
90 overnight cultures 1:20 in fresh LB without antibiotics and incubation for 4 h at 37°C. The  
91 cells were washed in PBS and 50 µl of resuspended pellets were used to infect mice *per os*  
92 (5x10<sup>5</sup> CFU). Competitions were performed by inoculating 1:1 mixtures of each competitor  
93 strain.



94 Feces were sampled daily, homogenized in 1 ml PBS by bead beating (3mm steel ball, 25 Hz  
95 for 1 minute in a TissueLyser (Qiagen)), and *S.Tm* strains were enumerated by selective  
96 plating on MacConkey agar supplemented with the relevant antibiotics. Samples for lipocalin-  
97 2 measurements were kept homogenized in PBS at -20 °C. At endpoint, intestinal lavages  
98 were harvested by flushing the ileum content with 2 ml of PBS using a cannula. The  
99 mesenteric lymph nodes, were collected, homogenized in PBS Tergitol 0.05% v/v at 25 Hz  
100 for 2 minutes, and bacteria were enumerated by selective plating.  
101 Competitive indexes were calculated as the ratio of relative population sizes of competitors at  
102 a given time point, normalized for the ratio in the inoculum.

103

#### 104 **Non-typhoidal *Salmonella* transmission**

105 Donor mice were vaccinated with PA-*S.Tm*<sup>ΔoafA ΔgtrC</sup> once per week for 5 weeks, streptomycin  
106 pretreated (25 mg streptomycin *per os*), and gavaged 24 hours later with 10<sup>5</sup> CFU of a 1:1  
107 mixture of *S. Tm*<sup>ΔoafAΔgtrCwzyB::cat</sup> (Cm<sup>R</sup>) and *S. Tm*<sup>ΔoafAΔgtrC Kan</sup> (Kan<sup>R</sup>). On day 4 post infection,  
108 the donor mice were euthanized, organs were harvested, and fecal pellets were collected,  
109 weighed and homogenized in 1 ml of PBS. The re-suspended feces (centrifuged for 10  
110 seconds to discard large debris) were immediately used to gavage (as a 50 μl volume  
111 containing the bacteria from on fecal pellet) recipient naïve mice (pretreated with 25 mg  
112 streptomycin 24 hours before infection). Recipient mice were euthanized and organs were  
113 collected on day 2 post transmission. In both donor and recipient mice, fecal pellets were  
114 collected daily and selective plating was used to enumerate *Salmonella* and determine the  
115 relative proportions (and consequently the competitive index) of both competing bacterial  
116 strains.

117

#### 118 **Quantification of fecal Lipocalin2**

119 Fecal pellets collected at the indicated time-points were homogenized in PBS by bead-beating  
120 at 25 Hz, 1min. Large particles were sedimented by centrifugation at 300 g, 1min. The  
121 resulting supernatant was then analysed in serial dilution using the mouse Lipocalin2 ELISA  
122 duoset (R&D) according to the manufacturer's instructions.

123

#### 124 **Analysis of IgA-coating, and O:5/O:12 expression on *S.Tm* in cecal content**

125 Fresh cecal content or feces was re-suspended in sterile PBS by bead-beating at 25 Hz, 1min  
126 (previously demonstrated to disrupt IgA cross-linked clumps(9)). An aliquot estimated to  
127 contain not more than 10<sup>6</sup> *S.Tm* was directly stained with a monoclonal human IgG-anti-O:12  
128 (STA5(9)) and biotin-conjugated anti-mouse IgA clone RMA-1 (Biolegend), and/or Rabbit-  
129 anti-*Salmonella* O:5 (Difco). After washing, secondary reagents Alex647-anti-human IgG  
130 (Jackson ImmunoResearch), Pacific Blue-conjugated streptavidin (Molecular Probes),  
131 Phycoerythrin-conjugated streptavidin (Molecular Probes) and/or Brilliant violet 421-anti-  
132 Rabbit IgG (Biolegend) were added. After a final washing step, samples were analysed on a  
133 BD LSRII flow cytometer, or a Beckman Coulter Cytoflex S, with settings adapted for  
134 optimal detection of bacterial-sized particles. The median fluorescence intensity of IgA  
135 staining on *S.Tm* was determined by "gating" on bacterial sized particles and calculating the  
136 appropriate median fluorescence corresponding to O:12 or O:5 staining FlowJo (Treestar,  
137 USA). Gates used to calculate the % of "ON" and "OFF" cells were calculated by gating on  
138 samples with known ON or OFF phenotypes.

139

#### 140 **Analysis of specific antibody titers by bacterial flow cytometry**

141 Specific antibody titers in mouse intestinal washes were measured by flow cytometry as  
142 described(9, 51). Briefly, intestinal washes were collected by flushing the small intestine with  
143 5ml PBS, centrifuged at 16000 g for 30 min and aliquots of the supernatants were stored at -  
144 20°C until analysis. Bacterial targets (antigen against which antibodies are to be titered) were  
145 grown to late stationary phase or the required OD, then gently pelleted for 2 min at 3000 g.  
146 The pellet was washed with sterile-filtered 1% BSA/PBS before re-suspending at a density of  
147 approximately  $10^7$  bacteria per ml. After thawing, intestinal washes were centrifuged again at  
148 16000 g for 10 min. Supernatants were used to perform serial dilutions. 25  $\mu$ l of the dilutions  
149 were incubated with 25  $\mu$ l bacterial suspension at 4°C for 1h. Bacteria were washed twice  
150 with 200  $\mu$ l 1% BSA/PBS before resuspending in 25  $\mu$ l 1% BSA/PBS containing monoclonal  
151 FITC-anti-mouse IgA (BD Pharmingen, 10 $\mu$ g/ml) or Brilliant violet 421-anti-IgA (BD  
152 Pharmingen). After 1h of incubation, bacteria were washed once with 1% BSA/PBS and  
153 resuspended in 300 $\mu$ l 1% BSA/PBS for acquisition on LSRII or Beckman Coulter Cytoflex S  
154 using FSC and SSC parameters in logarithmic mode. Data were analysed using FloJo  
155 (Treestar). After gating on bacterial particles, log-median fluorescence intensities (MFI) were  
156 plotted against antibody concentrations for each sample and 4-parameter logistic curves were  
157 fitted using Prism (Graphpad, USA). Titers were calculated from these curves as the inverse  
158 of the antibody concentration giving an above-background signal.

159

#### 160 **Flow cytometry for analysis of O:5, O:4 and O:12 epitope abundance on *Salmonella* in** 161 **cecal content, enrichment cultures and clonal cultures**

162 1 $\mu$ l of overnight cultures, or 1 $\mu$ l of fresh feces or cecal content suspension (as above) was  
163 stained with STA5 (human recombinant monoclonal IgG2 anti-O:12(9)), Rabbit anti-  
164 *Salmonella* O:5 or Rabbit anti-*Salmonella* O:4. After incubation at 4°C for 30 min, bacteria  
165 were washed once with PBS/1% BSA and resuspended in appropriate secondary reagents  
166 (Alexa 647-anti-human IgG, Jackson Immunoresearch, Brilliant Violet 421-anti-Rabbit IgG,  
167 Biologend). This was incubated for 10-60 min before cells were washed and resuspended for  
168 acquisition on a BD LSRII or Beckman Coulter Cytoflex S.

169

#### 170 **Live-cell immunofluorescence**

171 200  $\mu$ L of an overnight culture was centrifuged and resuspended in 200  $\mu$ L PBS containing 1  
172  $\mu$ g recombinant murine IgA clone STA121-AlexaFluor568. The cells and antibodies were  
173 co-incubated for 20 minutes at room temperature in the dark and then washed twice in 1 mL  
174 Lysogeny broth (LB). Antibody-labeled cells were pipetted into in-house fabricated  
175 microfluidic device(52). Cells in the microfluidic device were continuously fed S.Tm-  
176 conditioned LB(52) containing STA121-AlexaFluor568 (1  $\mu$ g/mL). Media was flowed  
177 through the device at a flow rate of 0.2 mL/h using syringe pumps (NE-300, NewEra  
178 PumpSystems). Cells in the microfluidic device were imaged on an automated Olympus IX81  
179 microscope enclosed in an incubation chamber heated to 37°C. At least 10 unique positions  
180 were monitored in parallel per experiment. Phase contrast and fluorescence images were  
181 acquired every 3 minutes. Images were deconvoluted in MatLab(53). Videos are compressed  
182 to 7 fps, i.e. 1 s = 21 mins.

183

#### 184 **HR-MAS NMR**

185 *S. Typhimurium* cells were grown overnight (~18h) a to late stationary phase. The equivalent  
186 of 11–15 OD<sub>600</sub> was pelleted by centrifugation for 10 min 4 °C and 3750 g. The pellet was  
187 resuspended in 10% NaN<sub>3</sub> in potassium phosphate buffer (PPB; 10 mM pH 7.4) in D<sub>2</sub>O and

188 incubated at room temperature for at least 90 min. The cells were then washed twice with  
189 PPB and resuspended in PPB to a final concentration of 0.2 OD<sub>600</sub>/μl in PPB containing  
190 acetone (final concentration 0.1% (v/v) as internal reference. The samples were kept on ice  
191 until the NMR measurements were performed - i.e. for between 1 and 8 h. The HR-MAS  
192 NMR spectra were recorded in two batches, as follows: S.Tm<sup>WT</sup>, S.Tm<sup>wbaP</sup>, S.Tm<sup>Evolved\_1</sup>,  
193 S.Tm<sup>Evolved\_2</sup> were measured on 16.12.2016, S.Tm<sup>OafA</sup> was measured on 26.7.17.

194

195 NMR experiments on intact cells were carried out on a Bruker Biospin AVANCE III  
196 spectrometer operating at 600 MHz <sup>1</sup>H Larmor frequency using a 4 mm HR-MAS Bruker  
197 probe with 50 μl restricted-volume rotors. Spectra were collected at a temperature of 27 °C  
198 and a spinning frequency of 3 kHz except for the sample of OafA (25 °C, 2 kHz). The <sup>1</sup>H  
199 experiments were performed with a 24 ms Carr–Purcell–Meiboom–Gill (CPMG) pulse-  
200 sequence with rotor synchronous refocusing pulses every two rotor periods before acquisition  
201 of the last echo signal to remove broad lines due to solid-like material(27). The 90° pulse was  
202 set to 6.5 μs, the acquisition time was 1.36 s, the spectral width to 20 ppm. The signal of  
203 HDO was attenuated using water presaturation for 2 s. 400 scans were recorded in a total  
204 experimental time of about 30 minutes.

205

#### 206 **O-Antigen purification and <sup>1</sup>H-NMR**

207 The LPS was isolated applying the hot phenol-water method(54), followed by dialysis against  
208 distilled water until the phenol scent was gone. Then samples were treated with DNase  
209 (1mg/100 mg LPS) plus RNase (2 mg/100 mg LPS) at 37°C for 2 h, followed by Proteinase K  
210 treatment (1 mg/100 mg LPS) at 60°C for 1 h [all enzymes from Serva, Germany].  
211 Subsequently, samples were dialyzed again for 2 more days, then freeze dried. Such LPS  
212 samples were then hydrolyzed with 1% aqueous acetic acid (100°C, 90 min) and ultra-  
213 centrifuged for 16 h at 4°C and 150,000 g. Resulting supernatants (the O-antigens) were  
214 dissolved in water and freeze-dried. For further purification, the crude O-antigen samples  
215 were chromatographed on TSK HW-40 eluted with pyridine/acetic acid/water (10/4/1000, by  
216 vol.), then lyophilized. On these samples, 1D and 2 D (COSY, TOCSY, HSQC, HMBC) <sup>1</sup>H-  
217 and <sup>13</sup>C-NMR spectra were recorded with a Bruker DRX Avance 700 MHz spectrometer (<sup>1</sup>H:  
218 700.75 MHz; <sup>13</sup>C: 176.2 MHz) as described(55).

219

#### 220 **Atomic force microscopy**

221 The indicated S.Tm strains were grown to late-log phase, pelleted, washed once with distilled  
222 water to remove salt. A 20 μl of bacterial solution was deposited onto freshly cleaved mica,  
223 adsorbed for 1 min and dried under a clean airstream. The surface of bacteria was probed  
224 using a Dimension FastScan Bio microscope (Bruker) with Bruker AFM cantilevers in  
225 tapping mode under ambient conditions. The microscope was covered with an acoustic hood  
226 to minimized vibrational noise. AFM images were analyzed using the Nanoscope Analysis  
227 1.5 software.

228

#### 229 **Methylation analysis of S.Tm clones**

230 For REC-Seq (restriction enzyme cleavage–sequencing) we followed the same procedure  
231 described by Ardissonne et al, 2016(56). In brief, 1 μg of genomic DNA from each S.Tm was  
232 cleaved with MboI, a blocked (5'biotinylated) specific adaptor was ligated to the ends and the  
233 ligated fragments were then sheared to an average size of 150-400 bp (Fasteris SA, Geneva,  
234 CH). Illumina adaptors were then ligated to the sheared ends followed by deep-sequencing

235 using a HiSeq Illumina sequencer, the 50 bp single end reads were quality controlled with  
236 FastQC (<http://www.bioinformatics.babraham.ac.uk/projects/fastqc/>). To remove  
237 contaminating sequences, the reads were split according to the MboI consensus motif (5'-  
238 ^GATC-3') considered as a barcode sequence using fastx\_toolkit  
239 ([http://hannonlab.cshl.edu/fastx\\_toolkit/](http://hannonlab.cshl.edu/fastx_toolkit/)) (fastx\_barcode\_splitter.pl --bcfile barcodelist.txt --  
240 bol --exact). A large part of the reads (60%) were rejected and 40% kept for remapping to the  
241 reference genomes with bwa mem(46) and samtools(57) to generate a sorted bam file. The  
242 bam file was further filtered to remove low mapping quality reads (keeping AS >= 45) and  
243 split by orientation (alignmentFlag 0 or 16) with bamtools(58). The reads were counted at 5'  
244 positions using Bedtools(59) (bedtools genomecov -d -5). Both orientation count files were  
245 combined into a bed file at each identified 5'-GATC-3' motif using a home-made PERL  
246 script. The MboI positions in the bed file were associated with the closest gene using  
247 Bedtools closest(59) and the gff3 file of the reference genomes(60). The final bed file was  
248 converted to an MS Excel sheet with a homemade script. The counts were loaded in RStudio  
249 1.1.442(61) with R version 3.4.4(62) and analysed with the DESeq2 1.18.1 package(63)  
250 comparing the reference strain with the 3 evolved strains considered as replicates. The counts  
251 are analysed by genome position rather than by gene. The positions are considered  
252 significantly differentially methylated upon an adjusted p-value < 0.05. Of the 2607 GATC  
253 positions, only 4 were found significantly differentially methylated and they are all located in  
254 the promoter of the *gtrABC* operon.

255

#### 256 ***gtrABC* expression analysis by blue/white screening and flow cytometry.**

257 About 200 colonies of *S.Tm*<sup>*gtrABC-lacZ*</sup> (strain background 4/74, (22)) were grown from an  
258 overnight culture on LB agar supplemented with X-gal (0.2 mg/ml, Sigma) in order to select  
259 for *gtrABC* ON (blue) and OFF clones (white). These colonies were then picked to start pure  
260 overnight cultures. These cultures were diluted and plated on fresh LB agar X-gal plate in  
261 order to enumerate the proportion of *gtrABC* ON and OFF siblings. The proportion of  
262 O:12/O:12-2 cells was analyzed by flow cytometry.

263

#### 264 ***In vitro* growth and competitions to determine *wzyB*-associated fitness costs**

265 Single or 1:1 mixed LB subcultures were diluted 1000 times in 200 µl of media distributed in  
266 96 well Black side microplates (Costar). Where appropriate, wild type *S.Tm* carried a plasmid  
267 for constitutive expression of GFP. To measure growth and competitions in stressful  
268 conditions that specifically destabilize the outer membrane of *S.Tm*, a mixture of Tris and  
269 EDTA (Sigma) was diluted to final concentration (4 mM Tris, 0.4 mM EDTA) in LB. The  
270 lid-closed microplates were incubated at 37°C with fast and continuous shaking in a  
271 microplate reader (Synergy H4, BioTek Instruments). The optical density was measured at  
272 600 nm and the green fluorescence using 491 nm excitation and 512 nm emission filter  
273 wavelengths every 10 minutes for 18 h. The outcome of competitions was determined by  
274 calculating mean OD and fluorescence intensity measured during the last 100 min of  
275 incubation. OD and fluorescence values were corrected for the baseline value measured at  
276 time 0.

277

#### 278 **Serum resistance**

279 Overnight LB cultures were washed three times in PBS, OD adjusted to 0.5 and incubated  
280 with pooled human serum obtained from Unispital Basel (3 vol of culture for 1 vol of serum)  
281 at 37°C for 1 h. Heat inactivated (56°C, 30 min) serum was used as control treatment.

282 Surviving bacteria were enumerated by plating on non-selective LB agar plates. For this,  
283 dilutions were prepared in PBS immediately after incubation.

284

### 285 **Modeling antigen switching between O12 and O12-2**

286

287 The aim of this modeling approach is to test whether a constant switching rate between an  
288 O12 and an O12-2 antigen expression state can explain the experimentally observed bimodal  
289 populations.

290

291 To this end, we formulated a deterministic model of population dynamics of the two  
292 phenotypic states as

293

$$\frac{dO_{12}}{dt} = (\mu O_{12} - s_{\rightarrow 12-2} O_{12} + s_{\rightarrow 12} O_{12-2}) * \left(1 - \frac{(O_{12} + O_{12-2})}{K}\right)$$

294

$$\frac{dO_{12-2}}{dt} = (\mu O_{12-2} + s_{\rightarrow 12-2} O_{12} - s_{\rightarrow 12} O_{12-2}) * \left(1 - \frac{(O_{12} + O_{12-2})}{K}\right),$$

295

296 where  $O_{12}$  and  $O_{12-2}$  denote the population sizes of the respective antigen variants,  $\mu$  denotes  
297 the growth rate, which is assumed to be identical for the two variants,  $K$  the carrying capacity,  
298 and  $s_{\rightarrow 12-2}$  and  $s_{\rightarrow 12}$  the respective switching rates from  $O_{12}$  to  $O_{12-2}$  and from  $O_{12-2}$  to  
299  $O_{12}$ . Growth, as well as the antigen switching rates, are scaled with population size in a  
300 logistic way, so that all processes come to a halt when carrying capacity is reached.

301

302 We use the model to predict the composition of a population after growth in LB overnight,  
303 and therefore set the specific growth rate to  $\mu = 2.05h^{-1}$ , which corresponds to a doubling  
304 time of roughly 20min. The carrying capacity is set to  $K = 10^9$  cells. We ran parameter scans  
305 for the switching rates  $s_{\rightarrow 12}$  and  $s_{\rightarrow 12-2}$ , with population compositions that start either with  
306 100% or 0%  $O_{12}$ , and measure the composition of the population after 16h of growth (**Fig.**  
307 **S4C**). The initial population size is set to  $10^4$  cells

308

309 Experimentally, we observe that when starting a culture with an  $O_{12}$  colony, after overnight  
310 growth the culture is composed of around 90%  $O_{12}$  and 10%  $O_{12-2}$  cells, whereas starting the  
311 culture with  $O_{12-2}$  cells yields around 50%  $O_{12}$  and 50%  $O_{12-2}$  cells after overnight growth  
312 (**Fig. S4B**). To explain this observation without a change in switching rates, we would need a  
313 combination of values in  $s_{\rightarrow 12}$  and  $s_{\rightarrow 12-2}$  that yield the correct population composition for  
314 both scenarios. In **Fig. S4D**, we plot the values of  $s_{\rightarrow 12}$  and  $s_{\rightarrow 12-2}$  that yield values of 10%  
315  $O_{12-2}$  (starting with 0%  $O_{12-2}$ , green dots) and 50%  $O_{12-2}$  (starting with 100%  $O_{12-2}$ ,  
316 orange dots). The point clusters intersect at  $s_{\rightarrow 12} = 0.144h^{-1}$  and  $s_{\rightarrow 12-2} = 0.037h^{-1}$  (as  
317 determined by a local linear regression at the intersection point).

318

319 We then used the thus determined switching rates to produce a population growth curve in a  
320 deterministic simulation, using the above equations for a cultures starting with 100%  
321  $O_{12-2}$ , (**Fig. S4E**, Left-hand graph) and for a culture starting with 0%  $O_{12-2}$  (**Fig. S4E**, right-  
322 hand graph).

323

324 These switching rates are consistent with published values (22). Our results show that the  
325 observed phenotype distributions can be explained without a change in the rate of switching  
326 between the phenotypes.



**Key to O-glycan repeat structures in this manuscript**

Serovar	Full Representation	SNFG Representation
<b>O:5,12</b>	<p style="text-align: center;"><b>O:5</b></p> <p style="text-align: center;">Abe(2--Ac) α1   3</p> <p style="text-align: center;">-2)-D-Man-(α1-4)-L-Rha-(α1-3)-D-Gal-(α1-</p> <p style="text-align: right;"><b>O:12</b></p>	
<b>O:4,12</b>	<p style="text-align: center;"><b>O:4</b> Abe α1   3</p> <p style="text-align: center;">-2)-D-Man-(α1-4)-L-Rha-(α1-3)-D-Gal-(α1-</p> <p style="text-align: right;"><b>O:12</b></p> <p style="text-align: right;"><b>O:12-2</b></p> <p style="text-align: right;">D-Glu α1   4</p>	
<b>O:5,12-2</b>	<p style="text-align: center;"><b>O:5</b></p> <p style="text-align: center;">Abe(2--Ac) α1   3</p> <p style="text-align: center;">-2)-D-Man-(α1-4)-L-Rha-(α1-3)-D-Gal-(α1-</p> <p style="text-align: right;"><b>O:12-2</b></p> <p style="text-align: right;">D-Glu α1   4</p>	
<b>O:4,12-2</b>	<p style="text-align: center;"><b>O:4</b> Abe α1   3</p> <p style="text-align: center;">-2)-D-Man-(α1-4)-L-Rha-(α1-3)-D-Gal-(α1-</p> <p style="text-align: right;"><b>O:12-2</b></p> <p style="text-align: right;">D-Glu α1   4</p>	

## Supplementary Figures 1 - 11

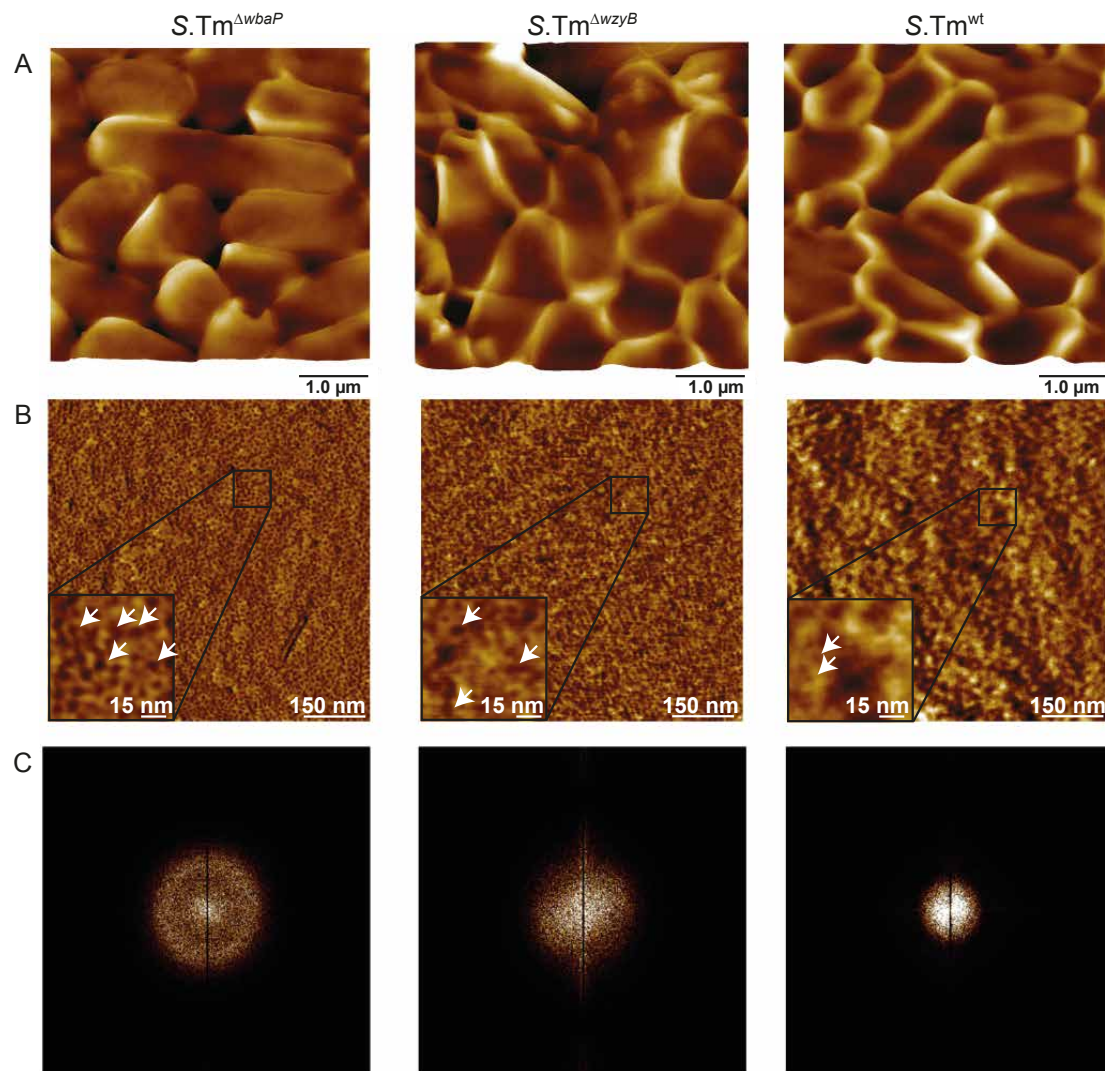


**Fig. S1: Surface phenotype of *S. Tm* mutants:** A-C. Atomic force microscopy phase images of *S. Tm*<sup>wt</sup>, *S. Tm*<sup>ΔwzyB</sup> (single-repeat O-antigen), and *S. Tm*<sup>ΔwbaP</sup> (rough mutant - no O-antigen) at low magnification (A) and high magnification (B and C). Invaginations in the surface of *S. Tm*<sup>ΔwbaP</sup> (dark colour, B) show a geometry and size consistent with outer membrane pores(64). These are already less clearly visible on the surface of *S. Tm*<sup>ΔwzyB</sup> with a single-repeat O-antigen, and become very difficult to discern in *S. Tm*<sup>wt</sup>. C. Fast-Fourier transform of images shown in "B" demonstrating clear regularity on the surface of *S. Tm*<sup>ΔwbaP</sup>, which is progressively lost when short and long O-antigen is present.

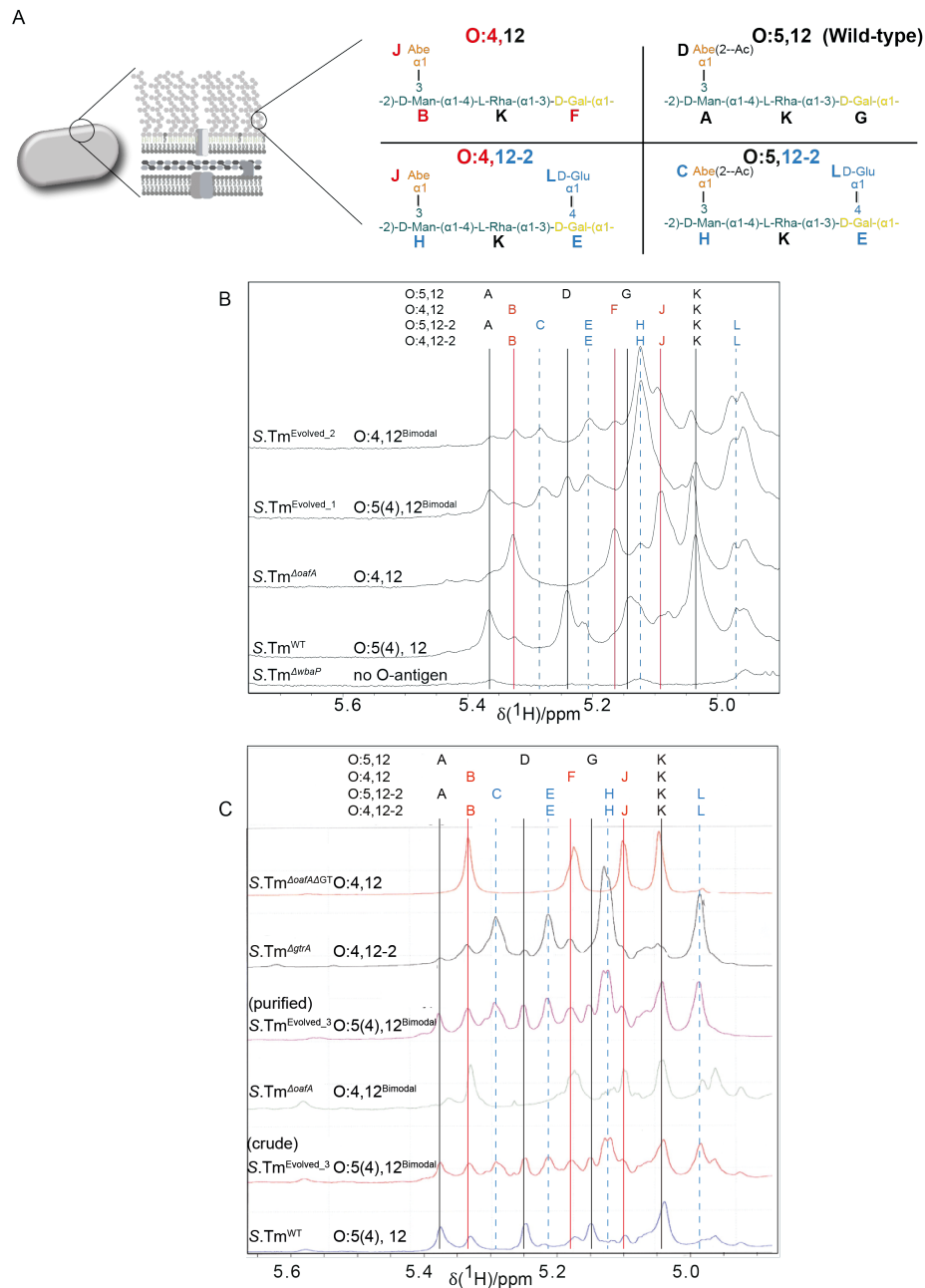


**Fig. S2: NMR of purified LPS from the indicated strains. A.** Schematic diagram of expected NMR peaks for each molecular species **B.** HR-MAS  $^1\text{H}$ -NMR spectra. Spectra show predicted peak positions, and observed spectra for C1 protons of the O-antigen sugars. **C.**  $^1\text{H}$  NMR of purified LPS from the indicated strains. Note that non-acetylated Abequose can be observed in wild-type strains due to spontaneous deacetylation at low pH in late stationary phase cultures(27). A *gtrA* mutant strain is used here to over-represent the O:12-2 O-antigen variant due to loss of regulation(31).

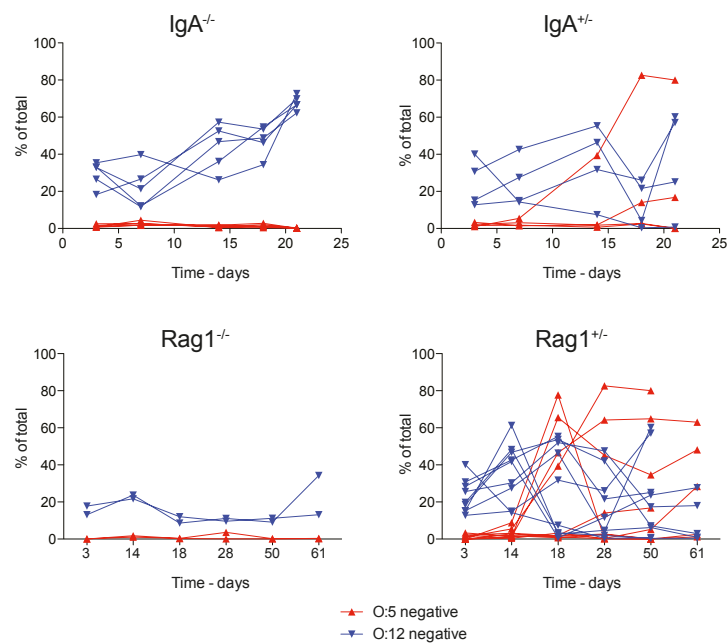


**Fig. S3: *S.Tm* O-antigen variation occurs in chronic *S.Tm* infections in an antibody-dependent manner.** IgA<sup>-/-</sup> and Rag1<sup>-/-</sup> and heterozygote littermate controls were pre-treated with streptomycin and infected with *S.Tm* <sup>$\Delta$ sseD</sup> orally. Feces were collected at the indicated time-points, enriched overnight in LB plus kanamycin, stained for O:5 and O:12 and analysed by flow cytometry. The fraction of the population that lost O:5 and O:12 antisera staining is shown over time. Outgrowth of O:12-negative *S.Tm* clones in IgA-deficient mice is likely due to weak compensatory responses from remaining adaptive immune mechanisms, e.g. IgM.

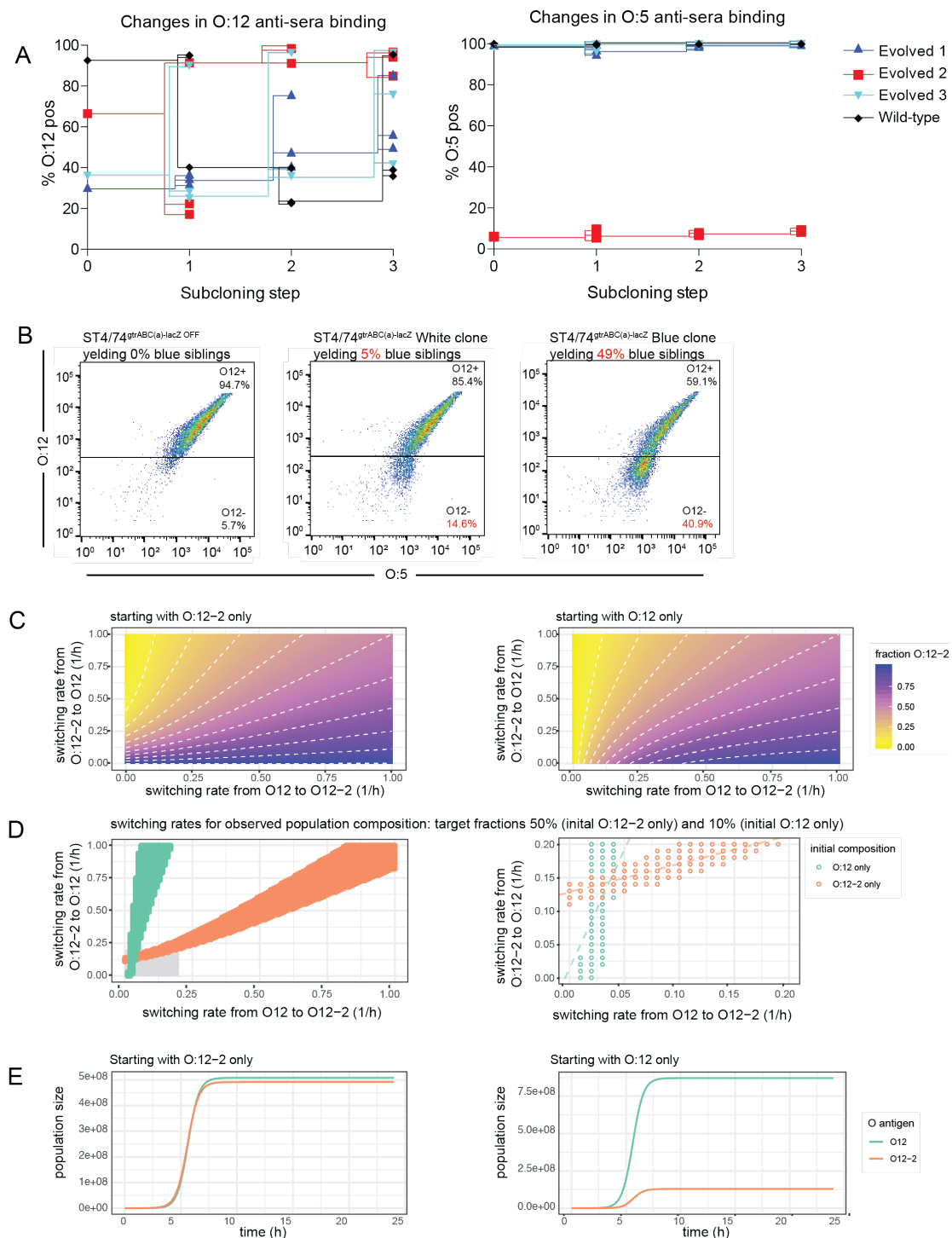


**Fig. S4: Loss of O:12-staining is a reversible phenotype.** **A.** Wild type and evolved *S.Tm* clones were picked from LB plates, cultured overnight, phenotypically characterized by O:12 (left panel) and O:5 staining (right panel), plated and re-picked. This process was repeated over 3 cycles with lines showing the descendants of each clone. **B.** Comparison of fractions of O:12-positive and O:12-negative bacteria (in fact O:12-2) determined by flow cytometry staining with typing sera and by blue-white colony counts using a *gtrABC-lacZ* reporter strain. **C-E.** Results of a mathematical model simulating bacterial growth and antigen switching. **C.** Switching rates from O:12 to O:12-2 and from O:12-2 to O:12 were varied computationally, and the fraction of O:12-2 was plotted after 16h of growth. Left-hand plot depicts the results of the deterministic model when starting with 100% O:12-2, right-hand plot depicts the results when starting with 100% O:12. **D.** depicts only the switching rates that comply with the experimentally observed antigen ratios after overnight growth (90% O12



when starting with O:12, and 50% O:12 when starting with O:12-2). Right-hand plot is a zoomed version showing values for switching rates between  $0 - 0.1 \text{ h}^{-1}$  (marked by a grey rectangle in **D**. left-hand plot). Dashed lines are linear regressions on the values in this range, and their intersection marks the switching rates used for the stochastic simulation in (E). **E**. Simulation results of bacterial population growth, when starting with only O:12-2 (left-hand plot) or only O:12 (right-hand plot).  $\mu = 2.05 \text{ h}^{-1}$  was kept constant in all simulations; switching rates were varied in steps of  $0.01 \text{ h}^{-1}$  in (C and D), and kept constant at  $s_{\rightarrow 12} = 0.144 \text{ h}^{-1}$  and  $s_{\rightarrow 12-2} = 0.0365 \text{ h}^{-1}$  in (E); the starting populations were always  $10^4 \text{ cells}$  individuals of the indicated phenotype; carrying capacity was always  $K = 10^9 \text{ cells}$ . Time resolution for the simulations is  $0.2 \text{ h}$ .



**Fig. S5: Mutations detected in the *oafA* gene sequence among several strains of *S. Tm* A.** Aligned fractions of the *oafA* ORF from a natural isolate (from chicken) presenting the same 7 bp deletion detected in mutants of *S. Tm* SL1344 emerging in vaccinated mice. *S. Tm* SL1344 was used a reference(65). **B.** Aligned *oafA* promoter sequences from three natural isolates of human origin (stool or cerebrospinal fluid(66)) showing variations in the number of 9 bp direct repeats.

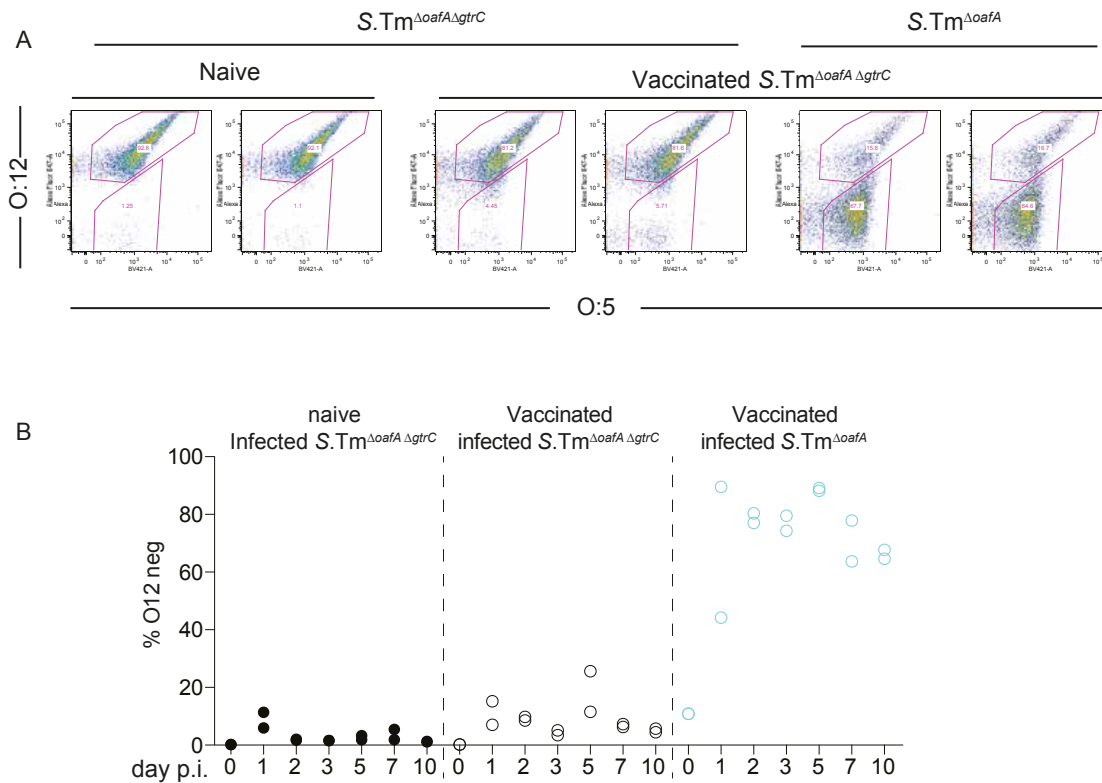


**Fig. S6: Glucosyltransferases containing loci including *gtrABC* are required for generation of the O:12<sup>Biomodal</sup> phenotype:** Wild type 129Sv mice were mock-vaccinated or were vaccinated with PA-*S.Tm* <sup>$\Delta$ oafA  $\Delta$ gtrC</sup> as in Fig. 1A. On d28, all mice were pre-treated with streptomycin, and infected with the indicated strain. A. Feces recovered at day 10 post-infection, was enriched overnight by culture in streptomycin, and stained for O:12. Fraction O:12-low *S.Tm* was determined by flow cytometry. Percentage of *S.Tm* that are O:12-negative was quantified over 10 days and is plotted in panel B.

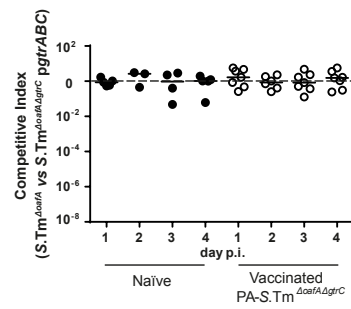


**Fig. S7: The  $\Delta gtrC$  mutation can be complemented in trans:** Mice were vaccinated and pre-treated as in **Fig. 3**. The inoculum contained a 1:1 ratio of  $S.Tm^{\Delta oafA}$  and  $S.Tm^{\Delta oafA} \Delta gtrC$  *pgtrABC*. Competitive index in feces was determined by differential selective plating over 4 days post-infection.

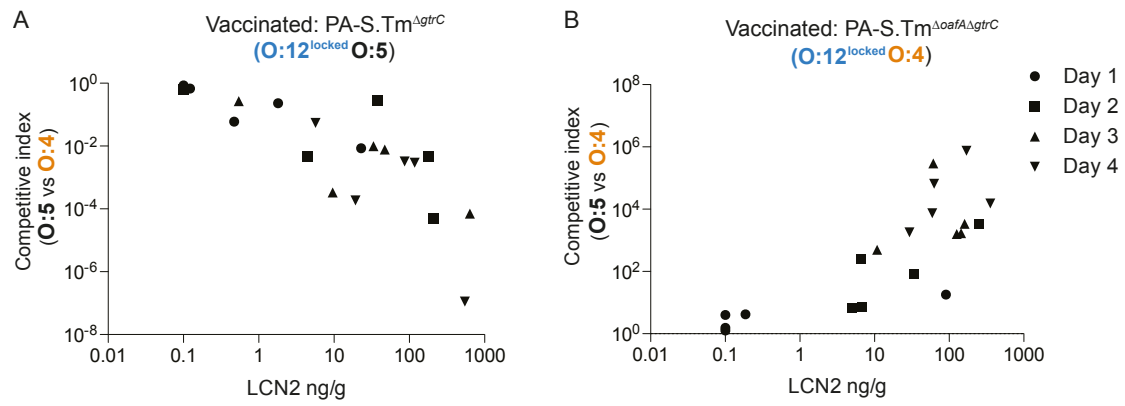


**Fig. S8: Fecal lipocalin-2 measurements corresponding to Fig. 3A.** Fecal Lipocalin 2 (LCN2) over days 1-4 plotted against the competitive index of infection for animals from Fig. 3A, vaccinated either against O:5-producing *S. Tm* (A), or O:4-producing *S. Tm* (B). Symbols indicate different days post-infection as indicated in the legend.



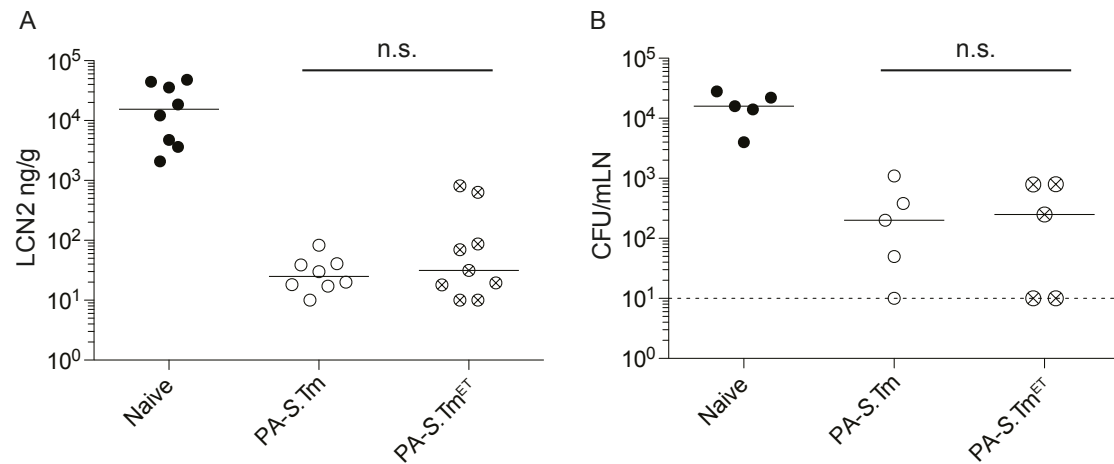


**Fig. S9: PA-STm<sup>ET</sup> does not significantly increase protection over a wild type vaccine at day 4 post-infection.** Mice were vaccinated with vehicle only (Naïve), PA-S.Tm<sup>wt</sup> or PA-STm<sup>ET</sup> (combined PA-S.Tm <sup>$\Delta$ grC</sup>, PA-S.Tm <sup>$\Delta$ oafA  $\Delta$ grC</sup>, PA-S.Tm *pgtrABC*, and PA-S.Tm <sup>$\Delta$ oafA</sup> *pgtrABC*, IgA titres shown in **Fig. 4A**). On day 28 after the first vaccination, mice were streptomycin pre-treated and challenged with 10<sup>5</sup> *S.Tm*<sup>wt</sup> orally. Fecal Lipocalin-2 (LCN2) at day 4 post-infection (**A**) and CFU *S.Tm*<sup>wt</sup> per mesenteric lymph node (MLN) at day 4 post-infection (**B**). Kruskal-Wallis analyses were carried out for significance.

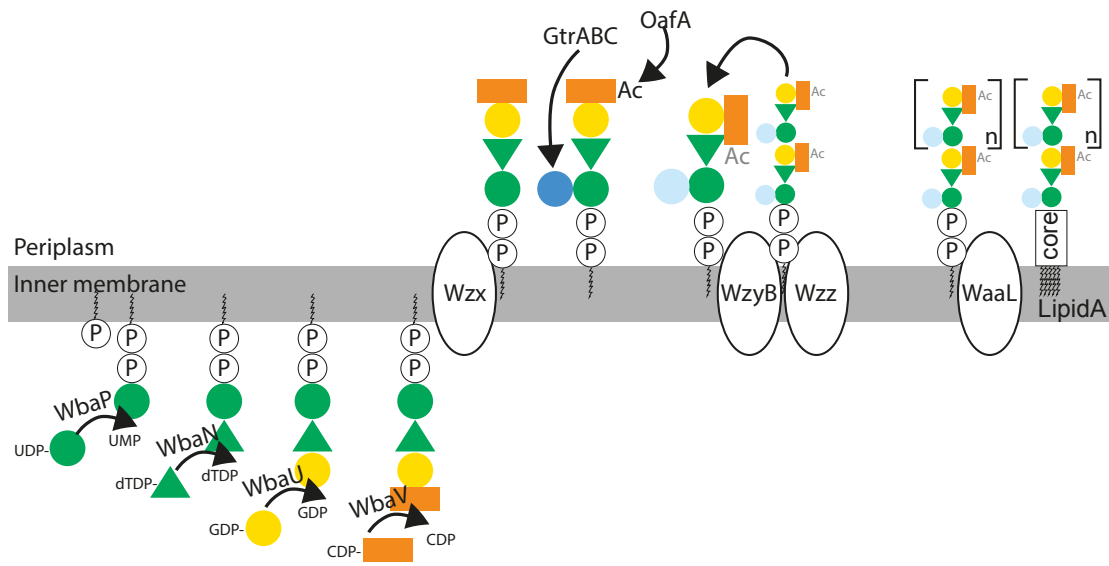


**Fig. S10: Schematic of *S. Tm* O-antigen synthesis (based on(67))**

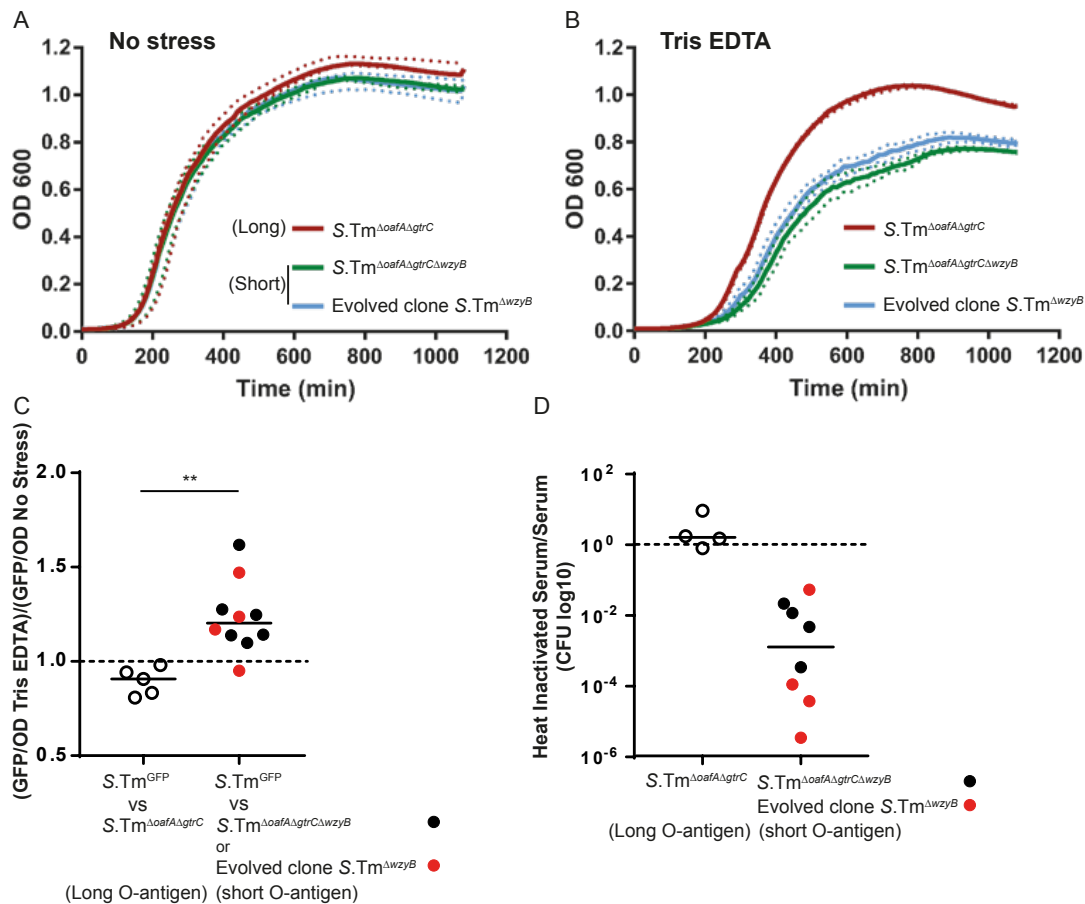


**Fig. S11 Synthetic and natural deletions of *wzyB* reduce the fitness of *S.Tm* in presence of Tris-EDTA and serum complement.** The deletion of *wzyB* does not affect the growth of *S.Tm* or  $S.Tm^{\Delta oafA \Delta gtrC}$  in LB (No stress) (A) but impairs growth in presence of Tris-EDTA (B). Dashed lines represent the range of variations between experiments. This was in line with the outcome of competitions between *S.Tm* expressing constitutive Green Fluorescent Protein ( $S.Tm^{GFP}$ ) and  $S.Tm^{\Delta oafA \Delta gtrC}$  or a *wzyB* mutant isolated from an Evoltrap vaccinated mouse (C). The level of GFP corrected for the optical density (OD) served as readout to quantify the  $S.Tm^{GFP}$  population at the end of the overnight growth, in presence of  $S.Tm^{\Delta oafA \Delta gtrC}$ ,  $S.Tm^{\Delta oafA \Delta gtrC \Delta wzyB}$  or an evolved  $S.Tm^{\Delta wzyB}$ , in LB with or without Tris-EDTA. Values above 1 (dashed line) indicates that relatively more GFP was detected in presence of Tris-EDTA than without, which resulted from a competitive advantage of  $S.Tm^{GFP}$  in presence of stress. D. The deletion of *wzyB* makes *Salmonella* sensitive to human serum complement. Values below  $10^0$  (dashed line) indicates that the number of colony-forming units (CFU) detected after incubation in human serum was lower than after incubation in heat inactivated human serum.

### **Supplementary Movies A and B**

Visualization of O:12 phase variation using live-cell immunofluorescence. Cells expressing GFP (green) pre-stained with fluorescently-labeled recombinant murine IgA STA121 specific for the O:12 epitope (red) were loaded into a microfluidic chip for time-lapse microscopy. Cells were fed continuously S.Tm-conditioned LB containing fluorescently-labeled recombinant murine IgA STA121 specific for the O:12 epitope. (A) Loss and (B) gain of antibody reactivity (red staining) was observed, indicative of O:12 phase variation.

**Supplementary Table 1: Strains and plasmids used in this study**

Strains	Background	Relevant genotype	Resistance*	Reference
<i>S.Tm</i> <sup>WT</sup>	SL1344	Wild-Type strain SB300	Sm	<i>Hoiseth 1981</i> (68)
<i>S.Tm</i> <sup><i>ΔsseD</i></sup>	SB300	<i>sseD::aphT</i>	Sm, Kan	<i>Hapfelmeier 2005</i> (69)
<i>S.Tm</i> <sup><i>ΔoafA</i></sup>	SB300	<i>ΔoafA Tag1::aphT</i>	Sm, Kan	This work
<i>S.Tm</i> <sup><i>ΔgrC</i></sup>	SB300	<i>grC(a)::cat</i>	Sm, Cm	This work
<i>S.Tm</i> <sup><i>ΔgrA</i></sup>	SB300	<i>grA(a)::cat</i>	Sm, Cm	This work
<i>S.Tm</i> <sup><i>ΔoafA ΔgrC</i></sup>	SB300	<i>ΔoafA grC(a)::cat</i>	Sm, Cm	This work
<i>S.Tm</i> <sup><i>ΔoafA ΔgrC kan</i></sup>	SB300	<i>ΔoafA grC(a)Tag1::aphT</i>	Sm, Kan	This work
<i>S.Tm</i> <sup><i>ΔoafA ΔgrC ΔwzyB</i></sup>	SB300	<i>ΔoafA grC(a) wzyB::cat</i>	Sm, Cm	This work
<i>S.Tm</i> <sup><i>ΔoafA ΔGT</i></sup>	SB300	<i>ΔoafA ΔgrB(a) ΔgrB(b) ΔSTM0712-0723 Δwca-wza</i>	Sm	This work
<i>S.Tm</i> <sup><i>grABC-lacZ</i></sup>	ST4/74	<i>grABC(a)-lacZ</i>		<i>Broadbent 2010</i> (22)
<i>S.Tm</i> <sup><i>grABC-lacZ OFF</i></sup>	ST4/74	<i>grABC(a)-lacZ</i> ; 3rd GTAC->GATA; 4th GATC->GATT		<i>Broadbent 2010</i> (22)
<i>S.Tm</i> <sup><i>ΔoafA ΔgrC pGrABC</i></sup>	SB300	<i>ΔoafA grC(a)::cat pGrABC</i>	Sm, Cm, Amp	This work
<i>S.Tm</i> <sup>GFP</sup>	SB300	Wild-Type strain SB300 pM965	Sm, Amp	This work
<b>Evolved clones</b>				
Evolved clone O:4,12	<i>S.Tm</i> <sup><i>ΔsseD</i></sup>	<i>sseD::aphT</i> ; clone R423A	Sm, Kan	This work
Evolved clone 1 O:5,12 <sup>Bimodal</sup>	<i>S.Tm</i> <sup><i>ΔsseD</i></sup>	<i>sseD::aphT</i> ; clone R421B	Sm, Kan	This work
Evolved clone 2 O:4,12 <sup>Bimodal</sup>	<i>S.Tm</i> <sup><i>ΔsseD</i></sup>	<i>sseD::aphT</i> ; clone R423B	Sm, Kan	This work
Evolved clone 3 O:5,12 <sup>Bimodal</sup>	<i>S.Tm</i> <sup><i>ΔsseD</i></sup>	<i>sseD::aphT</i> ; clone R430B	Sm, Kan	This work
Evoltrap evolved clones	<i>S.Tm</i> <sup>WT</sup>		Sm	This work
<b>Plasmids</b>	<b>Backbone</b>	<b>Relevant genotype</b>	<b>Resistance*</b>	<b>Reference</b>
pM965	pSC101	P <sub><i>rpsM</i></sub> - <i>gfp</i>	Amp	<i>Stecher 2004</i> (44)
p <i>grABC</i>	pM965	P <sub><i>rpsM</i></sub> - <i>grABC(a)</i>	Amp	This work
pKD46			Amp	<i>Datsenko 2000</i> (42)
pCP20			Amp, Cm	<i>Datsenko 2000</i> (42)
pKD3			Cm	<i>Datsenko 2000</i> (42)
* Relevant resistances only: Sm = ≥50 μg/ml streptomycin; Cm = ≥6 μg/ml chloramphenicol; Kan = ≥50 μg/ml kanamycin; Amp = ≥100 μg/ml ampicillin.				



## Supplementary Table 2: Primers used in this study

Primer name	Sequence	Purpose	Reference
oafA_Seq_up	CCGCCATAGTTACGTTTTG	Sequencing oafA	This work
oafA_Seq_dw	AAGCTATAGCATAAAAATAATTGC		This work
oafA_IntSeq1_up	AGTACTTGATTTTATATGCAAG		This work
oafA_IntSeq2_up	CAAGCTTATGGGATAGTCC		This work
oafA_IntSeq3_up	GCCTGATATTTGCTTCCTC		This work
oafA_IntSeq4_up	CCGTAATCTGAGAGATAATGA		This work
Del_oafA_up	AATTATAGGTAAAAAATGATCTACAAGAAATCAGACTCGTGTAGGCTGGAGCTGCTTC	In frame deletion oafA	This work
Del_oafA_dw	GCCAAGCCCTCTGTTTATTTGAAATCTGCTTTTCACTCATATGAATATCCTCCTTAG	This work	
Ver_oafA_up	ATGTAGTTGATGTAACAGGTC	Deletion verification oafA	This work
Ver_oafA_dw	ATGCCCATCAGAAAAGCT	This work	
Ver_STM0558_up	ATTGGTGTGATAAATCCTATTG	Deletion verification gtrC(a)	This work
Ver_STM0558_dw	GCTATCAGCCTGATATGCG		This work
Ver_STM4205_up	GTAATCATCAGAGTGAATAGG	Deletion verification gtrC(b)	This work
Ver_STM4205_dw	CGCAATTAGCCTTATTTGCG		This work
Del_wca_wza_up	TAAAAATAGCGGTACTTACCCTCCCGCTTCGGCAGCGAATGTAGGCTGGAGCTGCTTC	Deletion cluster wca-wza	This work
Del_wca_wza_dw	AGTGATAAATATCAATGATAATCCAAAATGAAATGACATATGAATATCCTCCTTAG	This work	
Ver_wca_wza_up	CCATAACATTAAGTATGAACAAC	Verification deletion cluster wca-wza	This work
Ver_wca_wza_dw	AAGCCGCTATTAAATTCACAA	This work	
Del_0712-23_up	TGATGGATTTGTTTTGAAAAGAAAATATCTACGCAAGTGTGTAGGCTGGAGCTGCTTC	Deletion cluster SaltsV1_0712 to SaltsV1_0723	This work
Del_0712-23_dw	GGAATTAATGAGCGCTTAGTTATATTTGCCAAAATTTTCATATGAATATCCTCCTTAG		This work
Ver_0712-23_up	ATTAAGTCTATCATCAGTAT	Verification deletion cluster SaltsV1_0712 to SaltsV1_0723	This work
Ver_0712-23_dw	GCGGAGCCGCCAATAA		This work
Del_0559_up	CGACTAACGAGATTTTCATTTCCGCATCCCTAAAGACAATGTGTAGGCTGGAGCTGCTTC	In frame deletion gtrA(a)	This work
Del_0559_dw	CCGCTGATTTTCATATATGTTGAAGTTATTCGCTAAGTACACATATGAATATCCTCCTTAG		This work
Ver_0559_up	TAGAAAATAGTATCTGTGGCT	Verification deletion gtrA(a)	This work
Ver_0559_dw	GTATGTCTACACTCCAGAC		This work
Del_gtrC_up	ATAATTAAGAAATGAGAAAGAAAATGGTTAACAATAGATATATGTGTAGGCTGGAGCTGCTTC	In frame deletion gtrC(a)	This work
Del_gtrC_dw	TACATGAATGTTATTTAATTAATTTCCGTAATATTCATTCATATGAATATCCTCCTTAG		This work
Ver_gtrC_up	CGCCGTTACCCATTGG	Verification deletion gtrC(a)	This work
Ver_gtrC_dw	TTGATAGGAATAGGTATTTCTGG		This work
Del_wzyB_up	TTCTAAAGGCTCTATATGCTTATAATTTTCATACATTCATATGCTGTGCAGGCTGGAGCTGCTTC	In frame deletion wzyB	This work
Del_wzyB_dw	TTCCCGCGTATAACTTATTTATTTCTTAGTAAAACGAATCTCATATGAATATCCTCCTTAG		This work
Ver_wzyB_up	CCAACAAGCTTTACAGGAAC	Verification deletion wzyB	This work
Ver_wzyB_dw	GATTGAGAATATCTGCCAGA		This work
PstII_Gtr57.59_up	ATCGTACTGCAGATGTTGAAGTTATTCGCTAAGTA	Cloning gtrABC(a)	This work
EcoRV_Gtr57.59_dw	GTAATCGATATCGCGGGGAACATTAATATATAC		This work
SeqInt1_gtrABC	CATACATCCTCTATTAATCATC	Sequencing P <sub>rpsM</sub> -gtrABC(a)	This work
SeqInt2_gtrABC	ATCTCTTGTAGTTGATTAATTTCT		This work
SeqInt3_gtrABC	TAATTAAGATGAGAAAGAAAATGGT		This work
SeqInt4_gtrABC	CGTCTGGCTAAGCGC		This work
SeqInt5_gtrABC	CAGCTGTCTTACGCTTCAT		This work
SeqInt6_gtrABC	ATGAGCTGATATGCGGATT		This work

**Supplementary Table 3: Mutations detected in genome sequencing of O:12<sup>Bimodal</sup> clones**  
 Numbers in parentheses indicate the number of reads covering the indicated position in the genome.

Clone name Staining with O:5 antisera Staining with O:12 antibody Serotype	Ancestor				Evolved (Chronic infection, day 36)				Reference	Allele	Region	Function
	R423A Negative Positive	R421B Positive Bimodal	R423B Negative Bimodal	R430B Positive Bimodal	O:4,12 Positive Bimodal	O:5,12 [12-21] Positive Bimodal	O:4,12 [12-2] Negative Bimodal	O:5,12 [12-2] Positive Bimodal				
	635606 (98)	635606 (97)	635606 (100)	635606 (99)	635606 (100)	635606 (100)	635606 (100)	13832..13843 (43)	GCGCGGATTT	-	<i>dnaJ</i>	Chaperone protein DnaJ
	1756092 (100)	1756092 (98)	1756092 (100)	1756092 (100)	1756092 (95)	1756092 (95)	1756092 (98)	T	A	STM0576	putative PTS system mannose-specific enzymes IIAB	
		2330274..2330280 (100)	2330274..2330280 (100)		2330274..2330280 (76)	2330274..2330280 (76)	2330274..2330280 (76)	ATTTTAT	-	<i>ycfT</i>	putative regulatory protein	
					2388693..2388694 (100)	2388693..2388694 (100)	2388693..2388694 (100)	TG	C	<i>oagA</i>	O antigen acetylase	
					2388696 (100)	2388696 (100)	2388696 (100)	C	A	Deletion <i>g/pA</i>	sh-glycerol-3-phosphate dehydrogenase subunit A	
	2411272 (100)	2411272 (99)	2411272 (100)	2411272 (99)	2411272 (100)	2411272 (100)	2411272 (100)	A	T	<i>merC</i>	o-succinylbenzoate synthase	
	2433677 (100)	2433677 (99)	2433677 (100)	2433677 (100)	2433677 (100)	2433677 (100)	2433677 (100)	T	G	<i>ruoF</i>	NADH-quinone oxidoreductase subunit F	
		2728584..2728589 (64)	2728584..2728589 (64)					GCAAGG	-	intergenic	Prophage Gifsy-1	
								C	T	<i>hilC</i>	Transcriptional regulator HilC	
								A	G	<i>tsr</i>	methyl-accepting chemotaxis protein I	
		4810885 (98)	4810885 (98)		4810885 (98)	4810885 (98)	4810885 (98)	G	A	<i>creD</i>	conserved exported protein of unknown function	
				4905774 (22)				T	G			